# The Magnetocaloric Effect in Hexagonal Laves Compounds

## How to substitute Scandium

F. J. le Roy
Studentnumber: 4009843
TU Delft department: Fundamental Aspects of Materials and Energy

# Content

# 1-Introduction

In our normal refrigerators compression of fluids is the driving force in establishing a temperature difference between the room and the cool box. This works pretty well, but has considerable disadvantages, like the toxic cooling fluids, noisiness, and a high energy consumption. Cooling by means of a magnetic field, could offer a more energy efficient and clean alternative. In fact the magnetic heat cycle is 35% more efficient than the vapor compression cycle[5]. Besides that the refrigerant material is solid, so it will not expell polluting gases into the atmosphere, as used to be a problem with the CFC's of oldfashioned refrigerators. In the vapor compression cycle, a phase change from liquid to gas induces a temperature difference, under adiabatic conditions. The magnetic refrigerator works the same, the only difference is that the refrigerant material in a magnetic refrigerator undergoes a magnetic phase change. For instance, the magnetic phase of the refrigerant material will change from the ferromagnetic to the paramagnetic state.

Magnetic refrigeration is already a common method to cool at very low temperatures. The first one to implement this technique was W. F. Giauque, who cooled helium down to 0.25K, using the adiabatic demagnetization of paramagnetic salts. Still a lot of research is being done on magnetic cooling at room temperature. Until now a few prototypes based on this technique have been realized [5]. The reason why magnetic cooling at room temperature is difficult is that the magnetized refrigerant needs to have a magnetic phase transition in the temperature range where the cooling is performed. Only then, materials can show a large magnetocaloric effect, the principle on which magnetic refrigeration is based. The temperature at which ferromagnetic materials become paramagnetic, the Curie temperature, is usually far above room temperature. At the same time materials with a phase change around zero Kelvin are available. The emergence of materials with a phase change around room temperature is more recent. In 1997 the discovery of the giant magnetocaloric effect by Pecharsky and Gschneider [2] in $Gd_5Si_2Ge_2$ set a new perspective for the magnetic refrigerator. The giant magnetocaloric effect (GMCE) is a first-order magnetic phase transition, it involves more dramatic changes than the conventional second-order phase transitions. This way, greater cooling power can be achieved. Since 1997 lots of materials with a phase change around room temperature have been investigated. Prof. E. Brück and his group from FAME mostly studied $Fe_2P$ based compounds exhibiting the giant magnetocaloric effect [3][4][4]. With these compounds a wine cooler has been built in cooperation with the BASF company [5]. To make magnetic cooling appealing for household refrigeration, the material should also be cheap and abundant, a request which further restricts the choice of elements and keeps the search for new materials ongoing.

The aim of this project is to look for a new magnetocaloric material inspired by the promising magnetic properties of $Fe_2Sc$ [6], in which scandium is the much too costly element thats needs an alternative.

## 1.1-The magnetocaloric effect

Magnetic refrigeration is based on the magnetocaloric effect (MCE), the phenomenon that ferromagnetic materials experience a reversible temperature change when they are exposed to a change in magnetic field at a temperature that is around their Curie temperature. Near the magnetic transition temperature the magnetization of the materials is reversible [7]. In the

temperature range where the material behaves ferromagnetic, once magnetized the material will never lose its magnetic ordering, as can be seen in the hysteresis loop. Thus in this range magnetization is mostly irreversible. Though, as long as the magnetization-temperature dependence has a slight slope, a small MCE can be induced. The first one to notice the magnetocaloric effect was Thomson (later known as Lord Kelvin) in 1860 [7]. He heated iron to the temperature where the ferromagnetic ordering disappears, it becomes paramagnetic around 770 °C, and saw that it became hotter when placed near to a magnet and colder when the magnet is removed. In 1907, Weiss and Picard, experimentally measured the effect with nickel, which has a lower Curie temperature than iron and therefore its temperature change was more easy to quantify. The first application of the MCE was sought in converting heat in electrical or mechanical power. Both Edison an Tesla patented a generator like this in the 1890s, but it was not commercially competitive. Magnetic refrigeration was invented in the 1920s by both Debey and Giauque. By demagnetizing paramagnetic salts, they found a way to cool below 1K.

There are three conditions for the MCE to manifest itself. A magnetic material at its magnetic transition temperature is needed to have a large effect, usually this is the Curie temperature where it changes from ferromagnetic to paramagnetic. Then there must be a changing magnetic field. And no heat exchange must occur during the transition, magnetization and demagnetizations must happen under adiabatic conditions. When the material is placed in the magnetic field its spin moments align, and due to this higher level of organization the magnetic entropy of the iron drops. Similarly when the field is removed, the material goes back to the paramagnetic phase with randomly orientated spins, and the magnetic entropy rises. However, since the transition from ferro- to paramagnetic is reversible and the process happens adiabatically, it is assumed that the total entropy remains constant [8]:

$$\Delta S(T,B) = \Delta S_m(T,B) + \Delta S_l(T,B) + \Delta S_e(T,B) = 0 \quad (1)$$

The magnetic entropy change, $\Delta S_m(T,B)$, and the related electronic entropy change, $\Delta S_e(T,B)$, are compensated by the entropy change $\Delta S_l(T,B)$ due to lattice vibrations, or phonons. If the material is magnetized, extra phonons are created and with them more lattice entropy to make up for the decrease in magnetic entropy. As a result the temperature of the material rises. Conversely, when the material is demagnetized and the magnetic entropy increases, phonons disappear and the temperature drops. This is the 'adiabatic temperature change'. It is proportional to the magnetic and electronic entropy which are called together the `isothermal entropy change'. So the aim is to maximize the isothermal entropy change.

This is the traditional way to explain the magnetocaloric effect. The mathematical model describing this effect is based on the assumption that the total entropy change is zero. This model is valid for the Brayton refrigeration cycle in which magnetization and demagnetization happen isentropically. In a spontaneous process entropy only increases, in accordance with the second law of thermodynamics. That the temperature rises, to compensate for the entropy loss if a material is magnetized, is natural. But this doesn't imply that the opposite, that an increase in entropy due to demagnetization is compensated by a decrease in entropy, is automatically true. So it should be emphasized that these are non-spontaneous processes. The mechanism that moves the refrigerant material away from the magnetic field, inducing the demagnetization and the corresponding cooling, consumes energy. The adiabatic condition is established by (de)magnetizing the refrigerant material

very quickly, leaving almost no time for heat to flow. Thus the mechanism that brings the material in and out of the field has to move fast, dissipating energy and increasing in the entropy in the environment outside of the closed refrigerant system. No violations of the second law are involved, after all. Of course the adiabatic and reversible assumptions, which provide together the isentropic assumption, are still idealized. The magnetization needs at least some time and the giant magnetocaloric effect usually involves a little hysteresis, meaning that it isn't entirely reversible.

## Thermodynamic description

### *Isothermal entropy change*

The thermodynamic equations underlying the magnetocaloric effect are derived from the Gibbs energy[8][9]:

$$G = U - TS + PV - MB \tag{2}$$

The internal energy changes for an internal energy transformation is:

$$dU = TdS - PdV + BdM \tag{3}$$

which makes the Gibbs free energy change as:

$$dG = VdP - SdT - MdB \tag{4}$$

the Maxwell relations are derived by letting the same variables independently change in a different order and set the second-order partial derivatives equal to each other. This way the Maxwell relation describing the MCE is calculated.

$$\left(\frac{\partial}{\partial B}\left(\frac{\partial G}{\partial T}\right)_B\right)_T = \left(\frac{\partial}{\partial T}\left(\frac{\partial G}{\partial B}\right)_T\right)_B \tag{5}$$

In constant pressure applies:

$$\left(\frac{\partial G}{\partial T}\right)_{B,P} = -S \tag{6}$$

$$\left(\frac{\partial G}{\partial B}\right)_{T,P} = -M \tag{7}$$

Inserting (6) and (7) in (5) gives the relevant Maxwell relation:

$$\left(\frac{\partial S}{\partial \mathrm{B}}\right)_{T,P} = \left(\frac{\partial M}{\partial T}\right)_{B,P} \tag{8}$$

This relation can be rewritten to give the isothermal entropy change, the entropy change due to the magnetic field which includes both $\Delta S_m(T, B)$ and $\Delta S_e(T, B)$.

$$dS_{iso}(T, \Delta B) = \int_{B_0}^{B_1} \left(\frac{\partial M}{\partial T}\right)_{B,P} dB \tag{9}$$

This equation holds when the material under consideration is homogeneous, in thermal equilibrium and the first derivative of the Gibbs free energy is continuous. Those three conditions are often not fulfilled for materials suitable for magnetic refrigeration, especially materials with a giant magnetocaloric effect [9]. For GMCE materials it is better to consider discrete changes in entropy and magnetization, using the Clausius-Clapeyron equation:

$$\Delta S_{iso} = -\Delta M / \left[\frac{dT_{tr}}{dB}\right]_p \quad (10)$$

in which $T_{tr}$ is the transition temperature.

### *The adiabatic temperature difference*

The isothermal entropy difference is proportional to the adiabatic temperature difference.

$$dT = -\frac{T}{C(T,B)} dS_{iso}(T, \Delta B) \quad (11)$$

In which C is the heat capacity:

$$C_x = \left(\frac{dQ}{dT}\right)_x = C_{B,P} = T\left(\frac{dS}{dT}\right)_{B,P} \quad (12)$$

Only, the heat capacity, $C_x = \left(\frac{dQ}{dT}\right)_x$, is discontinuous for first and second-order magnetic transitions, due to latent heat and because it is a second-order derivative of the free energy, respectively. Therefore equation (11) is not always valid [9]. However, the derivation now follows.

The total entropy change, which is zero, in the appropriate conditions, adiabatic and reversible, is:

$$dS = \left(\frac{dS}{dT}\right)_{B,P} dT + \left(\frac{dS}{dB}\right)_{T,P} dB = 0 \quad (13)$$

Inserting the expression for heat capacity in constant field and pressure $C_{B,P} = T\left(\frac{dS}{dT}\right)_{B,P}$ and the Maxwell relation $\left(\frac{dS}{dB}\right)_{T,P} = \left(\frac{dM}{dT}\right)_{B,P}$, (13) can be written as:

$$dS = \frac{C_{B,P}}{T} dT + \left(\frac{dM}{dT}\right)_{B,P} dB = 0 \quad (14)$$

Applying the isentropic condition and solving the equation gives the adiabatic temperature change.

$$dT_{ad} == -\frac{T}{C_{BP}(T,B)}\left(\frac{\partial M}{\partial T}\right)_{B,P} dB = -\frac{T}{C_{BP}(T,B)} dS_{iso}(T, \Delta B) \quad (15)$$

Equation (9) is used to relate the adiabatic temperature change to the isothermal entropy change.

## 1.2-Refrigeration Cycle

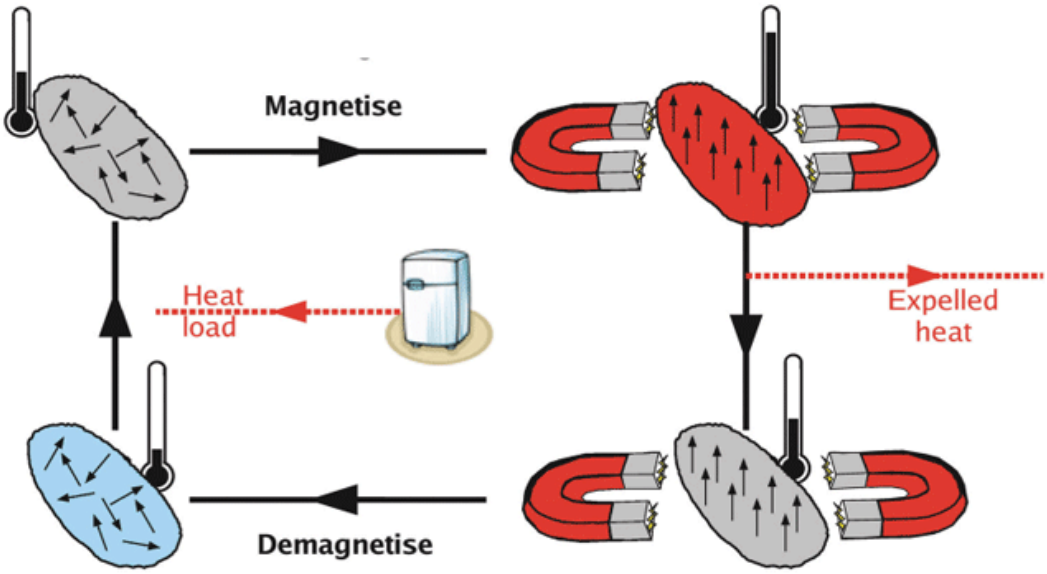


Figure 1: Schematic depiction of magnetic refrigeration retrieved from http://magnetocaloric.web.ua.pt/mce.html

In magnetic refrigerators, the fact that the magnetocaloric material cools down when it is demagnetized is used to build a refrigeration cycle, as shown in Figure 1. The heat that is created by magnetizing the material is released in the environment, then the material further cools because of demagnetization, so it can take up the heat from inside the coolbox. The thermodynamic equations above are relevant for the Brayton cycle, this is the cycle that is used for the wine cooler. It is depicted in Figure 2.

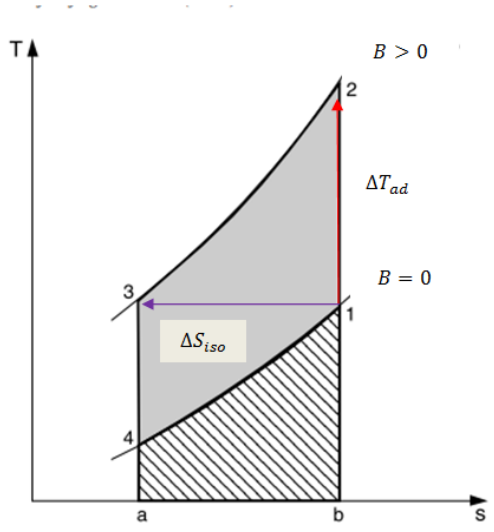


Figure 2: The Brayton refrigeration cycle

Magnetization and demagnetization happen isentropically, and heat is exchanged under isofield conditions. In step 1-2, the refrigerant is moved towards the magnet, experiencing an increase in field. It's temperature increases by the adiabatic temperature difference. In step 2-3 the refrigerant is in isothermal contact with the environment and expels the heat. Adiabatic demagnetization happens in step 3-4, by moving the refrigerant away from the magnet. The heat absorbed from the coolbox in step 4-1 is the striped area below the cycle:

$$\Delta Q = \int_4^1 T \Delta S_{iso} \qquad (16)$$

The greater the isothermal entropy difference the more cooling, that summarizes the thermodynamics of the magnetocaloric effect.

## 1.3-First and second-order phase transitions

Phase transitions are characterised by a discontinuity in the derivative of the Gibbs free energy with respect to field or temperature. If the first-order derivative is discontinuous, it is called a first-order phase transition. Likewise, if the second-order derivative is discontinuous, it is called a second-order phase transition [10]. The first-order magnetic phase transition is also called the Giant Magneto Caloric Effect (GMCE). In this type of transitions, the entropy, a first-order derivative of G with respect to temperature, and the magnetization, a first-order derivative with respect to the field are discontinuous. In case of a second-order magnetic transition, the first-order derivatives of G are zero, and the discontinuous second-order derivatives result in a jump in the magnetic susceptibility and heat capacity. The temperature were the transition happens is usually the Curie temperature $T_c$, were the material changes from ferromagnetic to paramagnetic. Other types of magnetic changes are also possible, for example, ferromagnetic to antiferromagnetic, in this case the transition is generally first-order.

### *Second-order phase transitions*

Second-order phase transitions are described by the Landau theory. In this theory the Gibbs free energy is expanded in a powerseries for the order parameter under consideration, the relative magnetization m in this case [11].

$$m = \frac{M(T)}{M(0)} \tag{17}$$

This is valid because the magnetization is small around the transition temperature $T_c$. Because the free energy is invariant for time reversal, only even powers are taken into account.

$$G(T, m) = G_0(T) + \frac{1}{2}A(T)m^2 + \frac{1}{4}B(T)m^4 \tag{18}$$

Or, in case of a magnetic field H, the free energy can be written as:

$$G(T, m) = -\mu_0 HM(0)m + G_0(T) + \frac{1}{2}A(T)m^2 + \frac{1}{4}B(T)m^4 \tag{19}$$

The free energy as a function of the relative magnetization is shown in Figure 3.

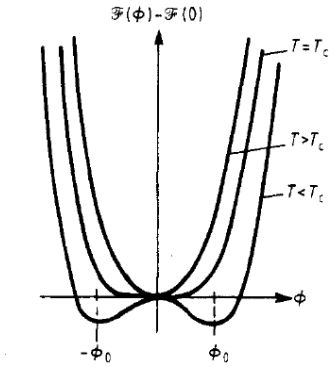


**Figure 3: Free energy (F=G) of an second-order magnetic transition as a function of the order parameter, ($\phi$ = m). copied from [12].**

In equilibrium the free energy should be minimal, which means that the first-order derivative is zero and the second-order derivative is positive:

$$\frac{\partial G}{\partial m} = 0 \tag{20}$$

$$\frac{\partial^2 G}{\partial m^2} > 0 \tag{21}$$

From these conditions, information about the constants can be deduced[11]:

$A(t) < 0 \; and \; B(t) > 0, \;\; for \; T < T_c$

$A(t) > 0, \;\; for \; T > T_c$

$$A(T) = a(T - T_c) \tag{22}$$

So the free energy is in zero field is:

$$G(T, m) = G_0 + \frac{1}{2}a(T - T_c)m^2 + \frac{1}{4}B(T)m^4 \tag{23}$$

From equation (29) and (32) the solution for the relative magnetization is found.

$$\text{For } T < T_c: m = \sqrt{\frac{a(T_c - T)}{B}} = \sqrt{\frac{-A}{B}} \tag{24}$$

$$\text{For } T = T_c: m = 0 \tag{25}$$

Inserting in this in the Gibbs free energy leads to:

$$G(T, m) = G_0 - \frac{1}{4}\frac{a^2(T_c - T)^2}{B} \tag{26}$$

As depicted in Figure 3. At the transition temperature, $T_c$ the Gibbs free energy is:

$$G(T_c, m) = Go + \Delta H - T\Delta S = G_0 \tag{27}$$

It can be seen that both the enthalpy change, $\Delta H$, and the entropy change are zero at the Curie temperature, since m is zero at the minimum of the free energy function ( see figure 3). This means that there is no latent heat, and the transition is truly reversible.

The second-order derivatives of the free energy with respect to field and temperature are respectivily susceptibility and heat capacity:

$$\chi = \frac{\partial M}{\partial H} = -\frac{\partial^2 G}{\partial H^2} \tag{28}$$

$$C = -T\frac{\partial^2 G}{\partial T^2} \tag{29}$$

Since the second derivative is discontinuous, the magnetic susceptibility goes to infinity at the Curie temperature, as depicted in Figure 4. Similarly, the heat capacity peaks around this temperature.

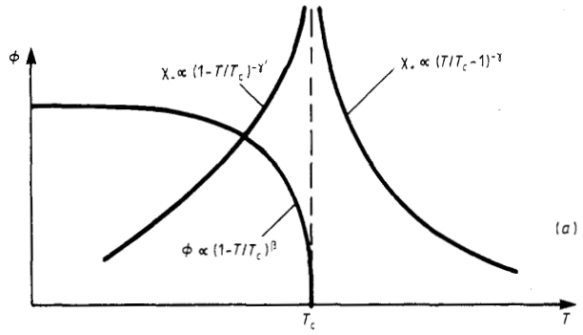


**Figure 4: The free energy $\phi$ and the magnetic susceptibility $\chi$ as a function of temperature, copied from [13].**

### *First-order phase transitions*

The Landau theory can also be used for first-order transitions. The free energy function is shown in Figure 5. At the transition temperature, $T_c$ in the figure, it has 3 minima at $Go$ . This implies that the order parmeter m, can jump from one minimum to the next, explaining the discontinuity in magnetization, the first derivative of G with respect to temperature.

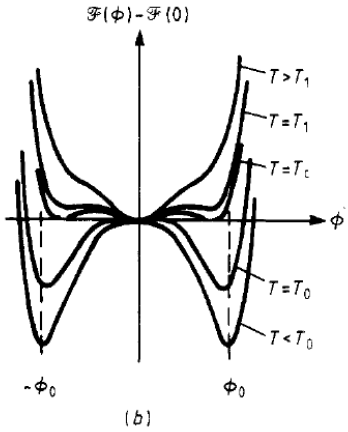


**Figure 5: Free energy of a first-order transition as a function of order parameter, copied from [13].**

In case of a first-order transition, the Gibbs free energy is approximated as:

$$G(T,m) = G_0 + \frac{1}{2}a(T-T_0)m^2 - \frac{1}{4}B(T)m^4 + \frac{1}{6}C(T)m^6 \tag{30}$$

At $T_c$ applies $G - G_0 = 0$, and the derivative $\frac{\partial G}{\partial m} = 0$, from these two equations the relative magnetization at the Curie temperature can be calculated [12][13]:

$$m = 0 \; or \; \mp\sqrt{\frac{3B}{4C}} \tag{31}$$

The magnetization can jump from $\mp\sqrt{\frac{3B}{4C}}$ to zero or vica versa. The change in magnetization brings along latent heat:

$$L(T_c, m) = T_c \Delta S = -\frac{1}{2} a T_c m^2 = -\frac{1}{2} a T_c \frac{3B}{4C} \tag{32}$$

Due to the jump in magnetization and magnetic entropy, more heat can be transferred with the giant magnetocaloric effect. But the application of the first-order magnetic phase transitions is less straightforward than of the second-order ones. Often hysteresis is present at the transition, meaning the magnetization field relation is different for field reversal, and thus a sign of irreversibillity.

## 1.4-Magnetism

### *Magnetic moment*

The magnetization of a material is the average of the magnetic moment of its atoms. The magnetic moment of an atom is:

$$\mu = g_j * \mu_B * J \tag{33}$$

$g_j$ is the Landé factor, it is a function of J, the total angular momentum quantum number and S, the spin angular momentum. $\mu_B$ means Bohr magneton: *'the electrons intrinsic magnetic moment'[26].* A Bohr magneton can be defined as the derivative of the classical Hamiltonian with respect to the magnetic field in the zero field limit [11], which gives:

$$\mu_B = \frac{e\hbar}{2m_e c} = 9.274 * 10^{-24} Am^2 \tag{34}$$

The total angular momentum quantum number J is a sum of the orbital angular momentum L and the spin angular momentum S. In the magnetic transition metals the orbital angular momentum can be neglected and J can be substituted by S. This so called quenching of the orbital magnetic moments happens because in transition metals the conduction electrons are delocalised from their nuclei. The electron wave functions are spread out and orbitals from different atoms combine. This is necessary to form bondings in metals, since the amount of nearest neighbours to bind is high compared to the number of valence electrons that can establish the bonding, so that atoms have to share their electrons. Due to the symmetry of the crystal structure the orbital angular momentum from the different atoms equals out to zero [14]. In magnetic rare earth metals though, the 4f electrons are very localised on their atoms, and the the orbital angular momentum does contribute. This is why rare earths can be stronger magnets [11]. Both cases, magnetism in 3d and 4f orbitals, have in common that since the orbitals are not filled a net angular momentum arises. In filled orbitals the spins of the electrons always add up to zero, and so does the total magnetization.

Materials with filled orbitals are diamagnetic, they only acquire a small magnetization opposite to the applied field due to the Lenz law [29].

### *Exchange Integral*

In ferro- ferri and antiferromagnetic materials interaction occurs between electrons of neighbouring atoms. The momenta of neighbouring atoms either try to align or disalign with each other, whichever is energetically favourable. How much energy the alignment of the momenta contributes to the total Hamiltonian of the interacting particles, is defined the Heisenberg Hamiltonian[26]:

$$H_{eff} = -2\sum_{i>j} J_{i,j} S_i \cdot S_j \tag{35}$$

In this equation it is assumed that the orbital moment can be neglected, and the interaction is just between the nearest neighbour atoms i and j. If i and j have parallel spins, $H_{eff} = -2J_{i,j}S^2$. Ferromagnetic materials are in favour of parallel spins, which means that the total energy is reduced by aligning spins, $H_{eff}$ is negative. Consequently the exchange integral $J_{i,j}$ of ferromagnetic materials is positive. Antiferromagnetic materials on contrary, in which spins tend to order antiparallel, have a positive exchange integral. If the particles are far apart, the exchange integral approaches zero and this is why only nearest neigbours are taken into account.

Coulomb interaction is the driving force which defines the sign of the exchange intergral, and the way particles interact. For a hydrogen molecule consisting of two hydrogen atoms which share their electrons it is energetically favourable to have both electrons in the orbital closest to the nucleus. To share the same s orbital, it is needed that they have opposite spins, because of the Pauli exclusion principle, and the exchange integral between the two electrons will be negative. In the 3d transition metals, e-e repulsion dominates, since the electrons are delocalised, and therefore far from the attractive nucleus. It is favoured when the electrons are further apart, and this is achieved with a repulsive exchange force, which is the result of an antisymmetric position wavefunction $\psi$(r) [15]. Since the overall fermion wavefunction $\psi$(r)$\psi$(s) must be antisymmetric, $\psi$(s) should be the symmetric triplet configuration, which means parallel spins. So for ferromagnetic transition metals the exchange force between electrons tends to align their spins as much as allowed by the Pauli exclusion principle.

Ferrimagnetic elements have an antiparallel ordering of moments but for one of the spin directions the moment is larger. In paramagnetic materials, the individual atoms still have a net moment but there is no magnetic ordering. They can be magnetised but have no spontaneous magnetization. All ferromagnetic materials and antiferromagnetic materials become paramagnetic at the Curie and the Néel temperature respectively. At this temperature the thermal energy $k_B T$ exceeds the Heisenberg hamiltonian, or the exchange energy [29]. For ferromagnetic materials the temperature dependance of the susceptibility is described by the Curie-Weiss law:

$$\chi = \frac{C}{T - T_c} \tag{36}$$

In which C is the Curie constant. For paramagnetic magnetic materials the formula is the same, just with $T_c = 0$. For antiferromagnetic materials $T_c$ is substituted by the negative material constant $\boldsymbol{\theta}$. The susceptibility is maximal at the Néel temperature, and then decreases because of the antiparallel ordering of the moments, it doesn't go to zero because of spincanting. Still a lot less field is necessary to magnetise antiferromagnetic compared to paramagnetic materials. The

magnetization-temperatue dependence of an antiferromagnetic material has the same shape as a ferromagnetic variant, only the magnetization will be lower. This is illustrated in the figures below.

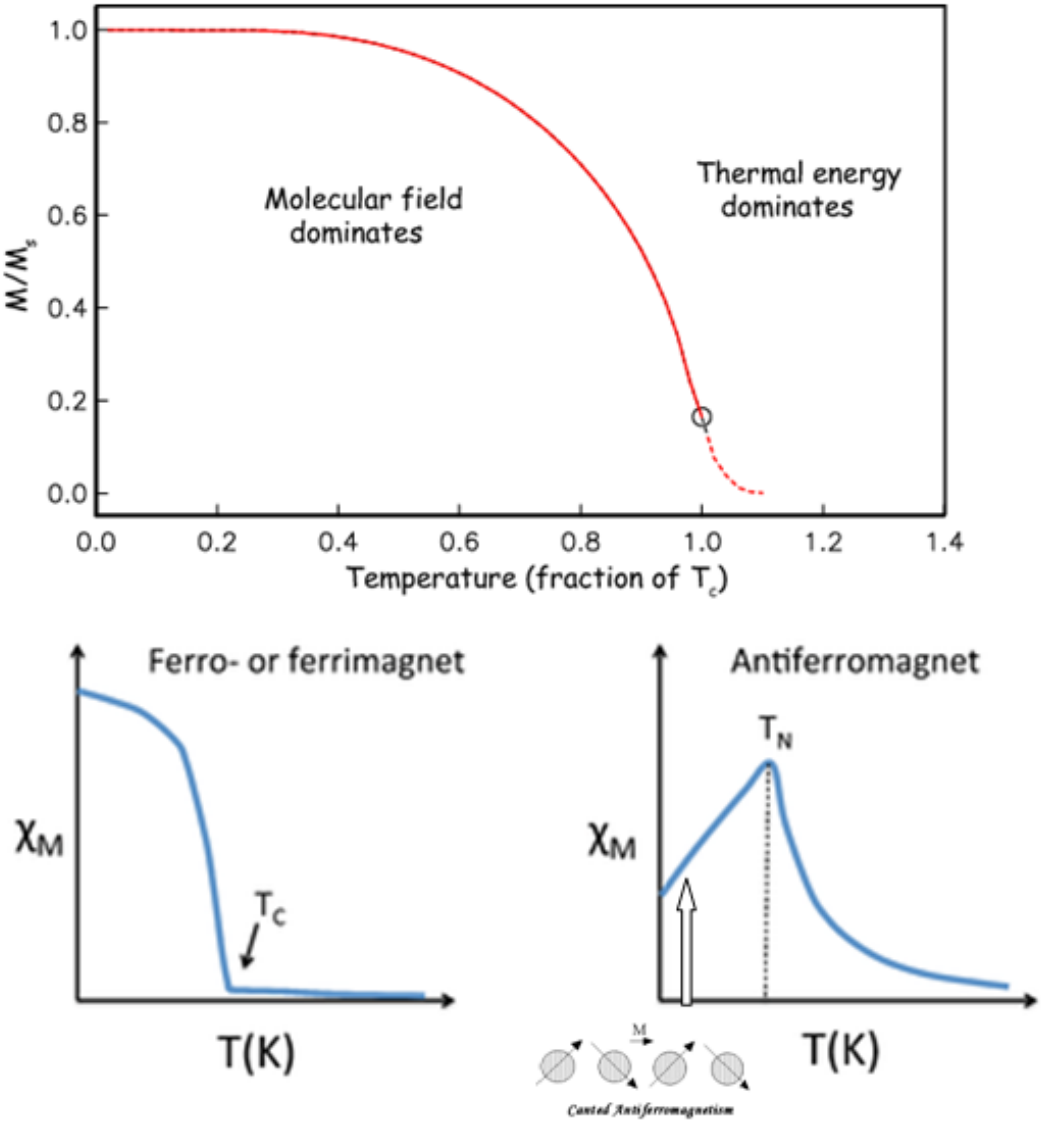


**Figure 6: Magnetization and susceptibility temperature depencies for ferro- and antiferromagnetic materials, copied from [30][31].**

### *Itinerant magnetism*

The magnetism in the 3d transistion metals is best described by the theory of itinerant magnetism. In this model, all valence electrons are treated as totally delocalized, free or travelling. Like in the free electon model, they fill up the available energy states upto the Fermi level. Since the 3d and 4s bands overlap in energy, the number of electrons in each band is not an round number. The number of electrons in the 4s band is in iron 2.2, in cobalt 1.7 and in nickel 0.6 [11]. In magnetic transition metals, the 3d orbital is not filled and can therefore have magnetic interactions. What kind of interactions depends on the crystal structure. To begin with, the general case of a positive exchange interaction is illustrated, which results in a ferromagnetic material.

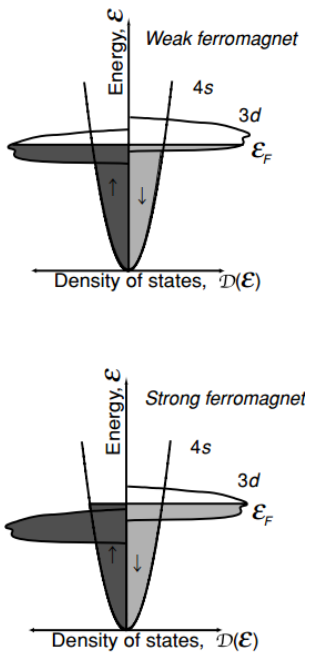


**Figure 7: Schematic density of states of a magnetic transition metal. On the left side are the spin up and on the right the spin down states. Copied from: 42[26]**

The iron atom acquires a maximimal magnetic moment if half of it's 8 valence atoms go to the 3d halfband with spin up and the other half divide between the 3d halfband with spin down and the 4s band. The 4s band is filled, so its spin moments are balanced, as can be seen from the density of states. If n is the number of valence electrons and x is the number of states in the 4s band, this results in a magnetic moment[11]:

$$\mu_H = (S\uparrow - S\downarrow)\mu_B = \left(\frac{n}{2} - \left(n - x - \frac{n}{2}\right)\right)\mu_B = (n - (n - x))\mu_B = x\mu_B \quad (37)$$

So the magnetic moment of an iron atom is $2.2\mu_B$, for cobalt 1.7 $\mu_B$ , and for for nickel it is $0.6\mu_B$.

These values agree with the experimental values. For compounds of the magnetic transition elements the same relation can be used [11], assuming that still the same number of 3d electrons moves to the 4s band. The fact that the band structure is different for a compound is neglected, therefore this way of calculating the magnetic moment is part of the rigid band model[33]. Only the total number of valence electrons $n_{total}$ changes because of the alloying, resulting in the similar formula below, which indeed works in practice for several alloys.

$$\mu_H = \left(\frac{n_{trans.metal}}{2} - \left(n_{total} - x - \frac{n_{trans.metal}}{2}\right)\right)\mu_B = (x + n_{trans.metal} - n_{total})\mu_B \quad (38)$$

Besides the itinerant theory of magnetism, there are also theories for magnetic coupling in which electrons are more localised. The magnetism of 4f rare earth elements are better described by a local theory, since 4f electrons don't have the task to establish bonding, and are close to the nucleus. To treat localised magnetism, other kinds of bonds than metal bonds must be taken into account, and the phenomena like the hybridization of different orbitals come into play.

## 1.5-Crystal structures

Since magnetism is about interactions between atoms, the crystal structure in which these atoms are connected is of major influence. It defines the number of nearest neighbours, or coordination number, the symmetry of the crystal lattice, the crystal field potential, it's filling factor and the interatomic distances.

In crystallography in total 7 crystal lattices are defined, based on their type of symmetry, like hexagonal or triclinic. These lattices are further specified in terms of symmetry operations and Bravais lattice amounting to a total of 230 types of crystal structures called spacegroups. Spacegroups can be denoted by their spacegroup symbol or spacegroup number, and are further subdivided in prototype compounds. For example spacegroup Fm3m, has spacegroup number 12 and one prototype is copper, it is the face centered cubic structure. Crystals from the same spacegroup have the same coordination number, and the same symmetry, resulting in similar physical properties. The crystal structure, denoted by the prototype compound defines the actual configuration of the atoms.

The relation between the number of valence electrons and nearest neighbours affects the material characteristics [27]. Diamonds are hard and insulating because carbon uses all it's four valence electrons for just four single bonds. Metals on contrary, often have much more nearest neighbours, a higher coordination number, than they have valence electrons to establish binding. Therefore they must share electrons and the electrons become delocalised between the atoms. This explains why metals are often ductile, why they conduct, why the free electron model and the itinerant theory of magnetism are a good approximation and why the electrons can easily interact with eachother, giving rise to (anti-)ferromagnetism. In a different crystal structures the same element can have different interactions. For example $\alpha$-Fe, having a bcc crystalstructure with 8 nearest neighbours, is usually ferromagnetic. Because of the electrons are delocalised to provide these bondings e-e repulsion will dominate, resulting in a positive exchange integral. Conversely $\varepsilon$-iron with an hcp stucture with only 6 nearest neighbours is often antiferromagnetic[28]. In this case there are more valence atoms available than there are bondings. So the electrons are more localised on the nucleus, giving rise to more degenerate energy levels and singlet configurations.

Since the 3d electrons cooperate in bonding, they aren't shielded from the crystal field potential, which is a function of all the charges in the material. A special case in which 3d electrons do act locally is therefore the crystal field splitting. This theory applies especially for interactions between 3d electrons and ligands, ions like $O^{2-}$. Due to the repulsion between electrons and the ligands, the 3d orbital splits in a lower energy antibonding orbital and a higher energy bonding orbital which forms a covalent bond with the 2p orbital of the ligand. The crystal structure affects the energy levels of this splitting. This illustrates the fact that 3d transition element can show metallic as well as covalent behavior, depending on the situations, which happens to be an important factor regarding the giant magnetocaloric effect.

### *Crystallographic roots of the giant magnetocaloric effect*

For the giant magnetocaloric effect some kind of chain reaction has to occur. For example changes in magnetization and crystal structure should reinforce eachother. Because the effect is caused usually by an interplay of different factors, finding the origin of this phenomenon is not easy. Different types of phase transitions have different causes.

The first-order magneto-elastic transition in $Fe_2P$-based compounds has now been explained by M. F. J. Boeije et al. [32]. In this compound, $(MnFe)_2(PSi)$, the ferromagnetic interaction takes place between iron and manganese atoms. At the transition temperature, which is around room temperature, this interaction dissapears, giving Fe electrons the oppurtunity to form a covalent bond with P and Si instead of aligning spins with Mn. The formation of the bond also induces the density of states to be more evenly distributed over the two spin bands, further decreasing the magnetization. So the nature of this phase transition is contributed to the ability of 3d electrons to form either magnetic moments or covalent bonds.

Different kind of first-order transitions are possible than the ferromagnetic to paramagnetic change, for example a change from ferromagnetic to antiferromagnetic ordering. Kittels model from 1960 [19] gives an explanation of such a phase change for $Mn_2Sb$ in terms of a balance between elastic and exchange energy. During the transition from the ferro- to the antiferromagnetic state, the lattice parameter c changes discontinuously, and Kittels model can predict this change in a quantitative way. The model starts, as usual, with the free energy, which is in this case a sum of the elastic energy and the magnetic exchange energy. The crystal lattice is split into two identical sublattices and the magnetic interaction is supposed to be between these two. The lattice parameter is dependent on thermal expansion, this is the elastic energy part, and it influences the interlattice interaction, since it defines the orientation of the sublattices. At the transition temperature the thermal equilibrium value of the lattice parameter reaches a critical value where the free energy is lowered by having antiparallel moments, and the material becomes antiferromagnetic. The difference in lattice parameter for the ferro and the antiferromagnetic state around this temperature is calculated by minimalizing the free energy. The change in c parameter is:

$$\Delta c = c_F - c_{AF} = \frac{2\rho M^2}{R} \tag{39}$$

In which M is the magnetic moment, R the elastic stiffness constant and $\rho = \frac{\partial \alpha}{\partial c}$, with $\alpha$ the mean field constant: $\alpha = \frac{2S^2}{k_B T} \sum_j J_{ij}$.

## 2-Research topic

The idea behind this project was to find new materials which could potentially be suitable for the magnetocaloric refrigeration. The current material, the $Fe_2P$-based compound, is already very good. However, to give possibilities for concurrence in an imaginairy 'magnetic refrigerator' market it is important to have multiple options for refrigerant materials. This is a reason to remain searching for new magnetocaloric materials.

BASF, the company that collaborates with Ekkes Brücks group in Delft and which is at the moment the only industrial company in this field, describes the requirements for a magnetocaloric material as follows [5]:

- *"High entropy change at phase transition*
- *Adiabatic (i.e., not releasing heat to the environment) temperature change in varying medium-strength magnetic fields*
- *Low thermal hysteresis resulting in low loss of heat*
- *Variable phase transition temperature*
- *Little volume change on phase transition*
- *High stability in operating conditions*
- *Raw material availability and security"*

For these cooling systems to be comercially competitive, also the production cost should be low. This means that the refrigerant material should be cheap, and that its entropy change should be large, to achieve great cooling power with relatively little refrigerant.

The aim of this project was not to meet all requirements above, just to look for a new compound which shows an interesting magnetic phase change and consist of relatively cheap elements. In this search was focussed on the hexagonal Friauf-Laves phase compounds, of which especcially the MgNi2 crystal structure seems promising. The Laves crystal structures are depicted in Figure 8. Crystal structures are referred to by their prototype compound, $MgNi_2$ and $MgZn_2$ in case of the hexagonal Laves phases, of spacegroup P63/MMC. The cubic $MgCu_2$ laves phase has spacegroup Fd 3m.

The Friauf-Laves crystal structures are related. If a the Laves compound is changed in stoichiometry it can easily go from one laves phase to the other. Looking at atomic positions, the $MgNi_2$ phase is most promising for the magnetocaloric effect, next comes the $MgZn_2$ phase, and the MgCu2 phase is least interesting. In iron compounds with a $MgNi_2$ structure, iron occupies as many as three different positions. That means the variety of interactions iron can have is relatively large. It can be that at a given temperature a ferromagnetic interaction dominates, and a higher temperature an antiferromagnetic or paramagnetic one. This could give rise to a magnetic transition. In the $MgZn_2$ structure, iron has two different positions and in the $MgCu_2$ phase just one.

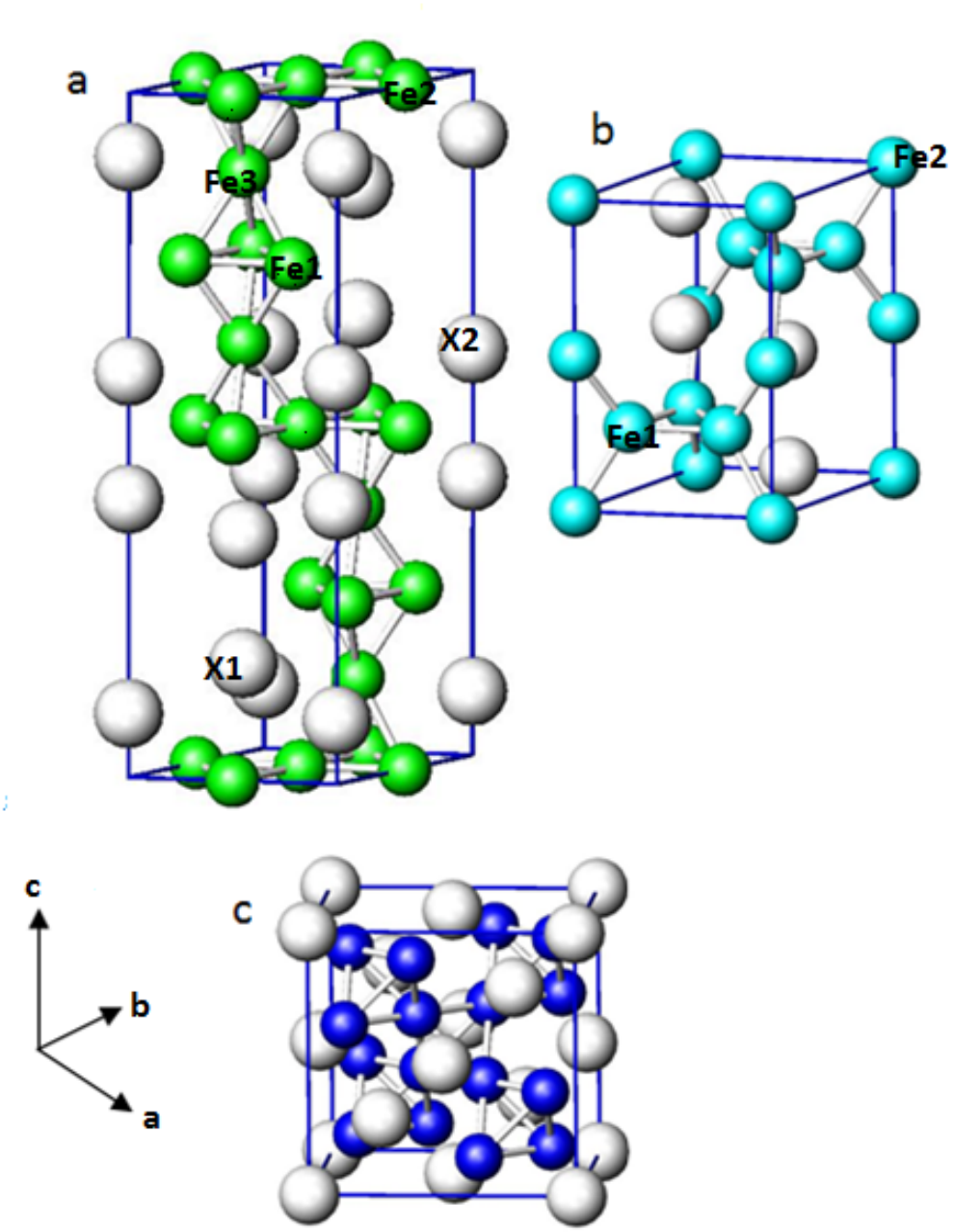


**Figure 8: The Laves crystal structures: a) C36 hexagonal Laves phase with prototype $MgNi_2$, b) C14 hexagonal laves phase with prototype $MgZn_2$, c) C15 cubic Laves phase phase with prototype $MgCu_2$. In the treated iron compounds, iron occupies the coloured sites.**

## 2-1 Magnetic transition in iron scandium compounds

Ironically, in this project, the inspiration for a new type of magnetocaloric materials was found in a paper on the properties of an iron compound with one of the most expensive elements on earth, scandium. Scandium costs currently €13 332 a kilo [17]. The paper, which reports on a magnetic phase transition in $Fe_2Sc$, is written in 1986 by Pokatilov et al. (in Russian, a translation is added in appendix A). It describes the magnetic properties of Fe – Sc compounds in different composition, and relates this to the crystal structure. The magnetic phase transition is found for the stoichiometric $Fe_2Sc$ and for compounds with a little excess in iron , containing 68.3% up till 75% iron. The magnetic phase transition is around 380 °C. Moreover, the compounds with extra iron, exhibit hysteresis, which is a sign of a first-order transition. The transition appears to be from ferromagnetic to antiferromagnetic. At least, this is deduced by the authors of the paper, comparing literature about similar transitions. The stoichiometric $Fe_2Sc$ compounds have a crystal structure of the cubic $MgCu_2$ type. The non-stoichiometric compounds, with the transition to antiferromagnetic phase, contain $Fe_2Sc$ in the hexaganal crystalstructure of the type $MgNi_2$ and $\alpha$-Fe. Pokatilov et al. seek the origin of the ferro- antiferromagnetic transition in the extra iron atoms that occupy 'wrong' sites in the lattice, sites which would belong to the scandium atoms in a stoichiometric composition. This way antiferromagnetic interactions between the iron atoms can arise. A comparison to the magnetic transition in $Fe_2Y$ spinglass [18] is made, were also the irregularities in the crystal structure provide competition between ferro and antiferromagnetic interactions. Also the temperature dependencies of the lattice parameters are investigated, lattice parameter c has a maximum around the transition temperature. In Kittels model [19], the relation between a discontinuous change in lattice parameter length and a ferro- antiferro magnetic transition is described. Whether the measured temperature dependency of c agrees with this theory is not stated in the paper though. The paper does mention that the $Fe_2Sc$ temperature dependency has great similarity with the material $Fe_2Hf_{(1-x)}Ta_{(x)}$ . This compound also has a ferro-antiferromagnetic transition [20]. The crystal structure is hexagonal, but of the $MgZn_2$ type instead of the $MgNi_2$ type. For both $Fe_2Sc$ and $Fe_2Hf_{(1-x)}Ta_{(x)}$ the phase change is considered best explained by the theory of Moriya and Usami [21] about antiferro- and ferromagnetism in itinerant electron magnets.

The phase change in $Fe_2Sc$ is remarkable, it is first-order, of the rare type ferro- to antiferromagnetic and at an high temperature, 380°C. Indeed the transition temperature is to high for the use in magnetic refrigerators, it is far above room temperature, but it is always possible to decrease this temperature by adding Mn to the composition. On the contrary, a way to increase the transition temperature hasn't been found yet. $YFe_2$ spinglass has a transition temperature around 53K, this is why it is not a suitable material for magnetic refrigerators, although yttrium is much cheaper than scandium. Also $Fe_2Hf_{(1-x)}Ta_{(x)}$ has a relatively low transition temperature, the transition only reaches room temperature at high contents of hafnium, which is a quite expensive element.

Another compound with a $MgZn_2$ structure, which has coexisting ferro- antiferromagnetic phases is the $Fe_2Ti$ compound with excess of $\alpha$-Fe[22][23]. The stoichiometric composition $Fe_2Ti$ is antiferromagnetic. But in non-stoichiometric compounds, where extra iron occupies the the titanium sites in the lattice, the extra iron interacts with otherwise paramagnetic iron atoms on the 2a sites of the lattice. This interaction results in a ferromagnetism that coexist with antiferromagnetism up to the transition temperature around 200K where the material becomes antiferromagnetic. The

magnetization gradually decreases until the Neél temperature around 300K[24]. All in all, the decrease in magnetization happens too continuously to be usefull for magnetic refrigeration.

This leads to the conclusion that from the currently known compounds with a ferro-antiferromagnetic transition, the Fe2Sc compound with a MgNi2 structure is the most suitable for magnetic refrigeration applications.

## 2-2 Substituting Scandium

Of course scandium is much too expensive to use as a refrigerant material. Even for further research, which is often based on trial and error, it is too costly. The aim is thus to substitute the Sc in $Fe_2Sc$ by one or more cheaper elements. The main parameters for a choice of elements are the crystal structure, $MgNi_2$, and the number of valence electrons.

Based on the number valence electrons, it is decided to substitute scandium by a half half mixture of titanium and magnesium. Titanium has one valence electron more than scandium and magnesium has one less, so together their number of valence electrons equals that of scandium. This simple argument is corroborated by the rigid band model for itinerant magnetism in compounds, which is also just based on the number of valence electrons.

For $Fe_2Sc$ there are 2 times 8 valence electrons of iron, and 3 valence electrons of scandium, assuming only iron contributes to the bonding gives:

$$\mu_H = (x + n_{trans.metal} - n_{total})\mu_B = (2 * 2.2 + 16 - 19)\mu = 1.4\mu_B \quad (40)$$

This magnetic moment agrees very well with the measurement of Pokatilov et all. for $Fe_2Sc$, which is $1.43\mu_B$. Therefore it is plausible that scandium can be substituted for something which has an equal number of valence electrons. Further more, it's hoped for that if the same number of valence bonds are available to form bondings, they will form the same crystal structure.

It is interesting that $Fe_2Ti$ already has a similar magnetic phase change from a ferromagnetic to a partly antiferromagnetic phase, with the same kind of explanation, iron occupying foreign sites. The other important factor is the crystal structure. $Fe_2Ti$ has a $MgZn_2$ structure, which is also of a hexagonal Laves phase, like $MgNi_2$. the $MgZn_2$ type structure is also contained by some Fe - Sc alloys. Expected is that the adding of magnesium makes the properties of the compound more similar to scandium, and therefore has a higher magnetization and transition temperature than $Fe_2Ti$. As a control an $Fe_2Ti$ sample will be replicated.

From the russian article can be concluded that the optimal Laves crystal structure is $MgNi_2$, which raises the question whether there are more compounds in the $MgNi_2$ crystal phase that have a magnetocaloric effect. All the compounds with a $MgNi_2$ structure that contain a magnetic transition metal are tabulated in the appendix B. Based on their magnetic properties and taking into account the abundance of contained elements, it is decided to investigate the YFeNi and $Fe_{70}Zr_{30}$ on this list, where zirkonium will be partly substituted by yttrium. These choices were inspired as well by the phase transition in $YFe_2$ spinglass, mentioned in the article. Yttrium is below scandium in the periodic table, indicating that it has very similar properties.

# 3-The Samples: methods and results

The first task is to make the compounds $Fe_2(MgTi)$, and FeNiY and $Fe_2(Y_x\ Zr_{1-x}\ )$Samples in the stoichiometric and in a non-stoichiometric composition will be made, analogous to the article on $Fe_2Sc$. Making the sample will be more challenging in the case of Fe-MgTi, which has never been made before. The basic principle in alloying metals is heating, this way the contribution of the mixing entropy to the total free energy increases, and therefore metals will tend to fuse into one crystal phase. If the melting temperature of the elements to be alloyed are similar, the arc-melter can be used. The arc-melter works like a welding device, it melts the metals together under argon atmosphere. This technique is used for preparing Fe-Ti, Fe-NiY and Fe-Zr-Y compounds. For the Fe-MgTi compounds the arc-melter can not be used because magnesium has a much lower melting point than Ti and Fe, even the vapor point is far below the melting point of the other two elements. Therefore these samples are prepared by mixing the powders first thoroughly, making use of a rotational ballmill device. In a rotational ballmill, little pots containing the ingredients and heavy balls are turned around real fast. Collisions between the balls and the ingredients provide the mixing. The pot and the balls are made from an extraordinairy hard material, wolfram carbide, to not pollute the sample. The heating of the Fe-MgTi samples is done by annealing them for a long time in the oven.

If the samples are ready, their crystalstructures will be measured with X-ray diffraction (XRD), and analysed by Fullprof Rietveld-refinement. This indicates if the elements have reacted, and in the optimal case, that their crystal structure is $MgNi_2$. If the samples have attained a single crystal phase, some useful conclusions can be drawn, even if this isn't the right phase. When the samples consist of multiple phases it is to complicated to analyse them further. The last step is to measure the magnetization temperature dependances, this is done with the SQUID magnetometer (superconducting quantum interference device), which measures up to 100°C. All SQUID measurements are done in a field of 1T. Phase transitions up to 450°C can be observed with another device called DSC (differential scanning calorimeter) which measures the heat capacity. A phase transition (not just a magnetic phase transition but all) is shown as a peak in the heat capacity. Magnetometers that can measure at high temperatures do exist, one such a device is located in Utrecht. But for none of the samples was necessary to travel all the way there. In fact none of the samples formed the $MgNi_2$ phase.

## 3.1-Stochiometic and non-stochiometric compounds of $Fe_2Ti$

To begin with, it was decided to first make $Fe_2Ti$ in it's stoichiometrical from and with extra Fe. This has been done already by Pelloth et al.[24], who also explain the nature of the magnetic phase transition in these compounds. But it is useful to see whether we can replicate their results. XRD and SQUID measurements are shown below.

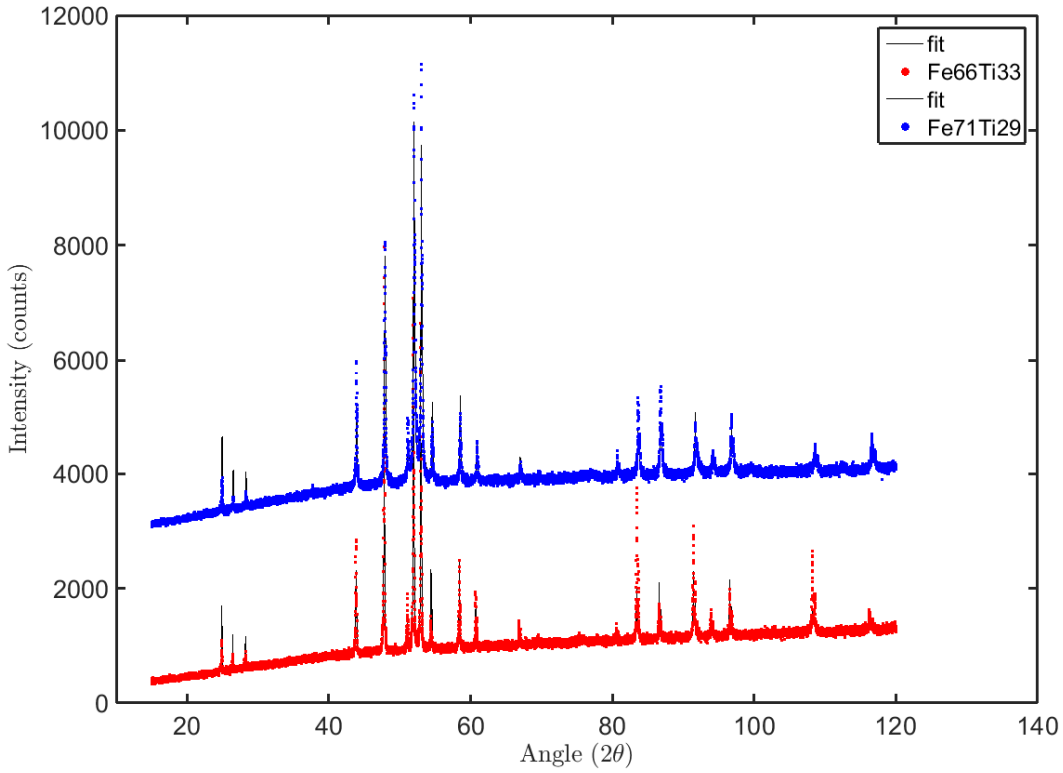


Figure 9: X-ray Diffraction spectrum of $Fe_2Ti$

| $Fe_{71}Ti_{29}$ | $\chi^2$ = 4,42 | | | $Fe_{66}Ti_{33}$ | $\chi^2$ = 4,56 | | |
|---|---|---|---|---|---|---|---|
| Phase | % | a&b | c | Phase | % | a&b | c |
| $MgZn_2$ | 100 | 4.785 | 7.803 | MgZn2 | 100 | 4.793 | 7.825 |

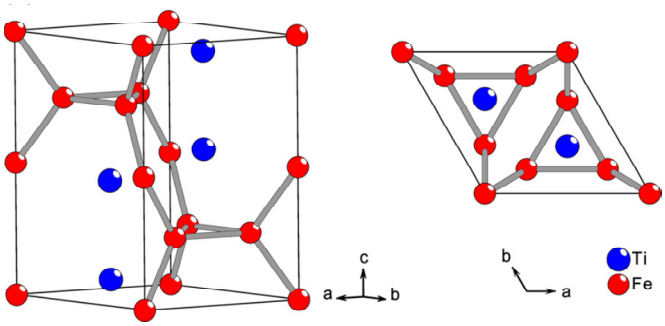


Figure 10: Ti and Fe in the $MgZn_2$ structure

From fullprof analyses of the occupancies of the lattice positions of Fe in $Fe_{66}Ti_{33}$ compound it was found that some extra iron was present, the compound was not exactly stoichiometric. The occupancies showed that iron from the 2a sites (the sites at the edges of the unit cell) moved to the titanium 4f sites (blue in Figure 10). This is in accordance with the Pelloth's paper. The iron on 6h

sites behave antiferromagnetically and the iron on 2a site is paramagnetic, but when the percentage iron becomes greater than 68% a ferromagnetic interaction arises between the 2a site iron atoms and the iron atoms occupying titanium sites. The result is that the stoichiometric compound of $Fe_2Ti$ is antiferromagnetic with a the Néel temperature around 300K. The compound with excess iron is weakly ferromagnetic up till 200K, after which ferromagnetic and antiferromagnetic states coexist, until the compound becomes paramagnetic as well at 350K. This is illustrated by the SQUID measurements.

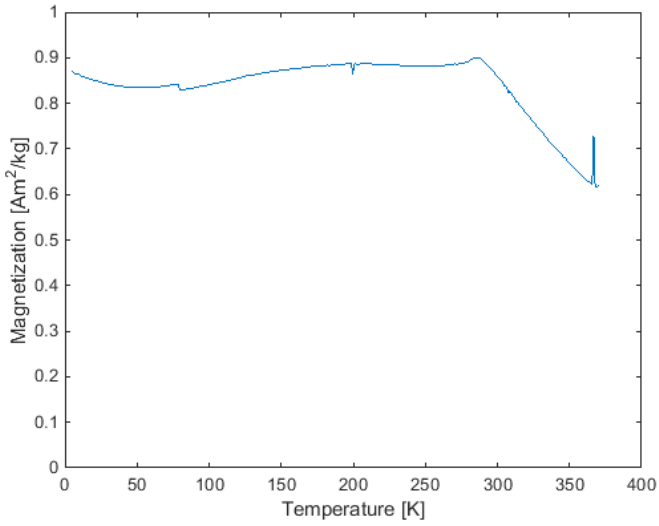


**Figure 11: Magnetization-temperature dependence of $Fe_{67}Ti_{33}$ , measured in a field of 1T.**

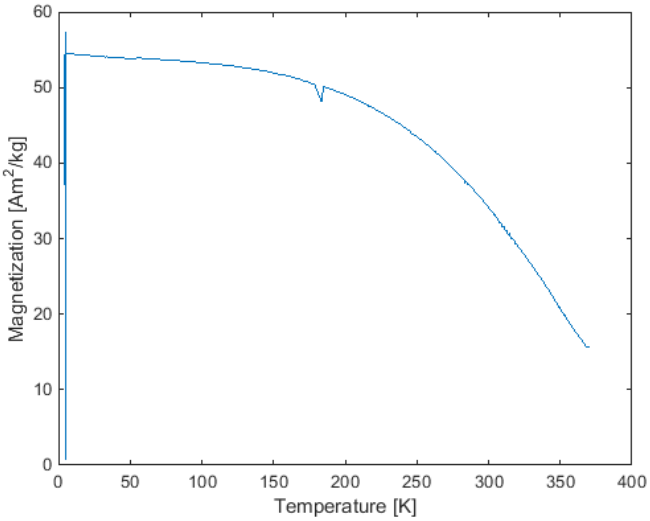


**Figure 12: Magnetization-temperature of $Fe_{71}Ti_{29}$, measured in a field of 1T**

In the stoichiometric compounds there seem to be strange curves around 100K, but taken into account that the magnetization is very low, this are only small fluctuations. Also the up going line at the right of the plot is probably just a measurement error. The peak at 300K coincides probably with

the Nèel temperature, where the susceptibility is at its maximum. The non-stoichiometric compound has clearly a much higher magnetization. It is remarkable though that both compounds have a small gap at 200K, where the transition from ferromagnetic to coexisting ferro- and antiferromagnetic states is supposed to begin.

## 3.2-Attempts to make Fe-MgTi compounds

$Fe_2Ti$ could easily be made, by arc melting. Adding magnesium is problematic though. The vapour point of magnesium (1091 °C) is below the melting point of iron (1538 °C) and titanium (1668 °C). The dilemma in making Fe-MgTi compounds is to let iron and titanium react without evaporating the magnesium.

The first strategy was to first mix titanium and magnesium by ball milling, hoping that they form a compound with a higher melting point, that could react with iron. Later it was tried to mill all three elements together, and anneal them in the oven.

### *Mixing Magnesium and Titanium*

Rousselot et al. made a 50% compound of Mg and Ti by ball milling it for 20 hours in a vibrational miller. A new fcc crystal phase formed between the elements. Based on the method of Rousselot et al Mg and Ti were combined in a 50% mixture and milled in rotational miller for 16 hours on 230 rpm. Intervals of 5 minutes milling and 5 minutes stopping are applied to keep the temperature below the vapour point of magnesium. A vibrational miller has a lot less G-force than a rotational one, so putting it 16 hours in the machine instead of 20 is supposed to make up for this difference. Per pot 8 milling balls of wolfram carbide were used, weighting around 8 grams a ball.

This first attempt failed because granules of Mg and Ti were used. The XRD diffraction spectrum matches mostly with pure Mg instead of a TiMg mixture. Most probably the titanium has been driven to the edges of the milling pot by centrifugal forces. The yield was around one half, the unrecoverable material, titanium apparently, adhered to the milling pot.

| | Mass [gr] |
|---|---|
| Ti | 2,653 |
| Mg | 1,347 |
| total | 4 |

| | sample 1 | sample 2 |
|---|---|---|
| Yield % | 65.9 | 64.6 |

| Phase | Sample 1 &2 | a&b | c |
|---|---|---|---|
| Mg (close-packed structure) | 100% | 3.208 | 5.210 |

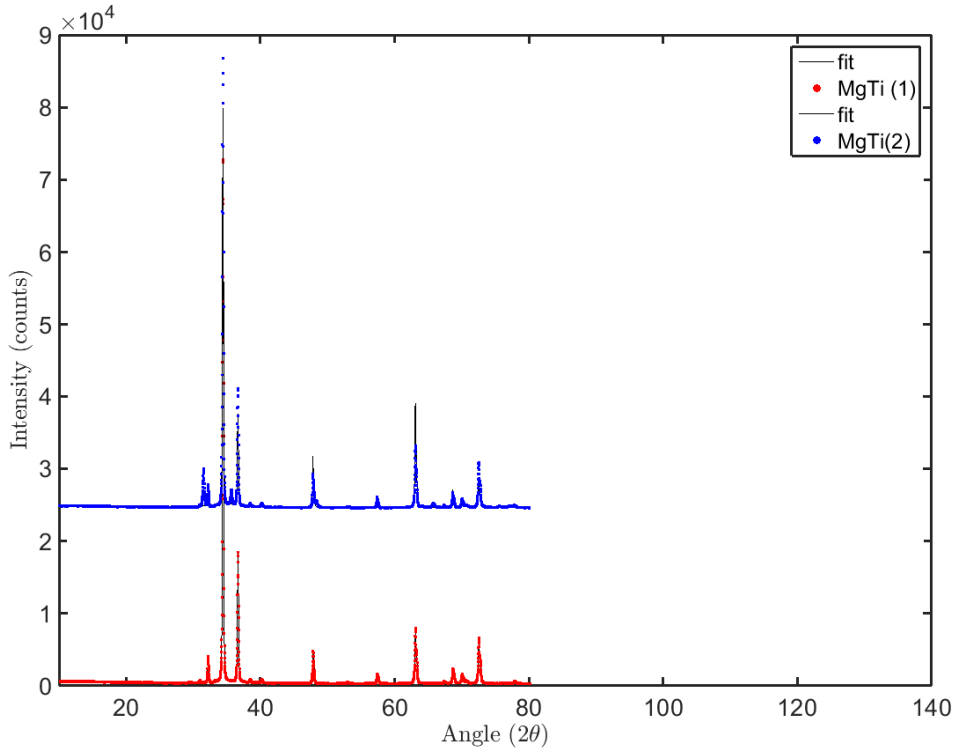


Figure 13: XRD spectrum of MgTi after milling granules for 16 hours

The ballmilling was repeated with powders. This resulted in a better yield, and not that dirty milling pots. After 10 hours of milling magnesium and titanium hadn't reacted yet, the mixture contained:

58% Magnesium
26% Titanium
16% $Mg_{0.6}Ti_{0.4}$

$\chi^2$ = 28.84

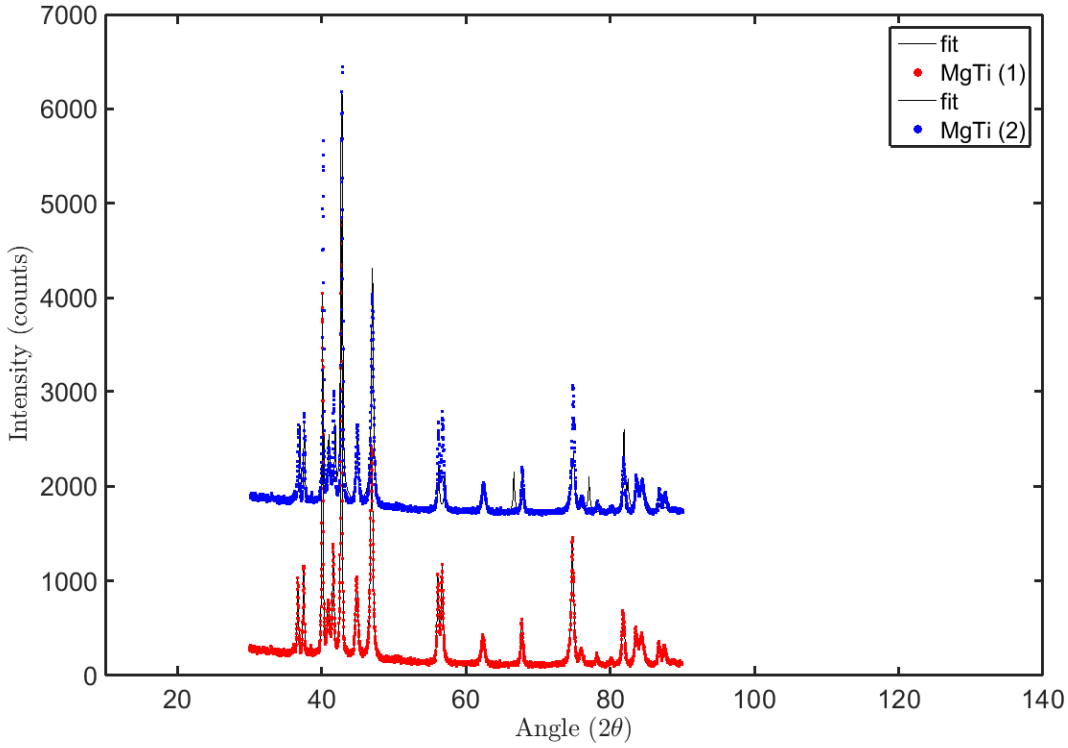


Figure 14: XRD spectrum of MgTi after milling powders for 10 hours

It was decided to mill for 70 hours more. This time, one of the pots had a yield higher than 100%, it appeared that part of the milling pots had solved into the sample. Peaks from wolfram carbide can be found in the diffractogram.

| | sample 1 | sample 2 |
|---|---|---|
| Yield % | 0.894 | 1.106 |

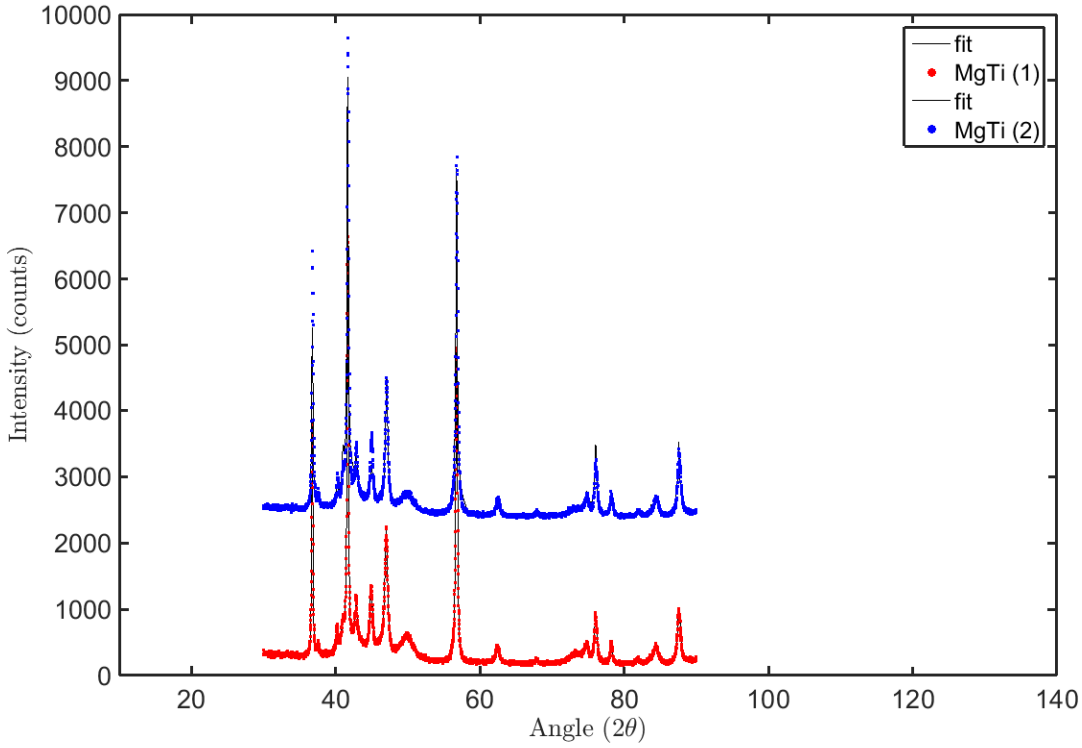


Figure 15: XRD of the MgTi sample milled for 80 hours and containing wolfrom carbide

| | MgTi (80h) s1 $\chi^2$ = 9.22 | | | MgTi (80h) s2 $\chi^2$ = 9.22 | | |
|---|---|---|---|---|---|---|
| | **fraction** | **lattice parameters** | | **fraction** | **lattice parameters** | |
| **phase** | **%** | **a & b** | **c** | **%** | **a & b** | **c** |
| **Mg** | 23 | 2.947 | 4.676 | 19.89 | 3.203 | 5.200 |
| **Ti** | 30.25 | 2.947 | 4.676 | 42.75 | 2.947 | 4.676 |
| **WC** | 40.74 | 2.904 | 2.836 | 37.36 | 2.904 | 2.836 |

These samples were mixed with iron by ballmilling for one hour. Longer was impossible, since the ballmill was broken by now. The mixed powder samples were compressed into pellets and sealed in quarts tubes filled with argon to prepare them for heat treatment. Then the samples were put into the oven to anneal for 1 week. Unfortunately, the oven behaved strangely that week and went up three times to 1300 °C. The tubes exploded and the samples came out burned.

### *Mixing iron magnesium and titanium*

This time we milled iron, magnesium and titanium for 4 hours at maximum speed: 380 rpm. Before the annealing already some Laves phases begin to form, especially the cubic $MgCu_2$ phase.

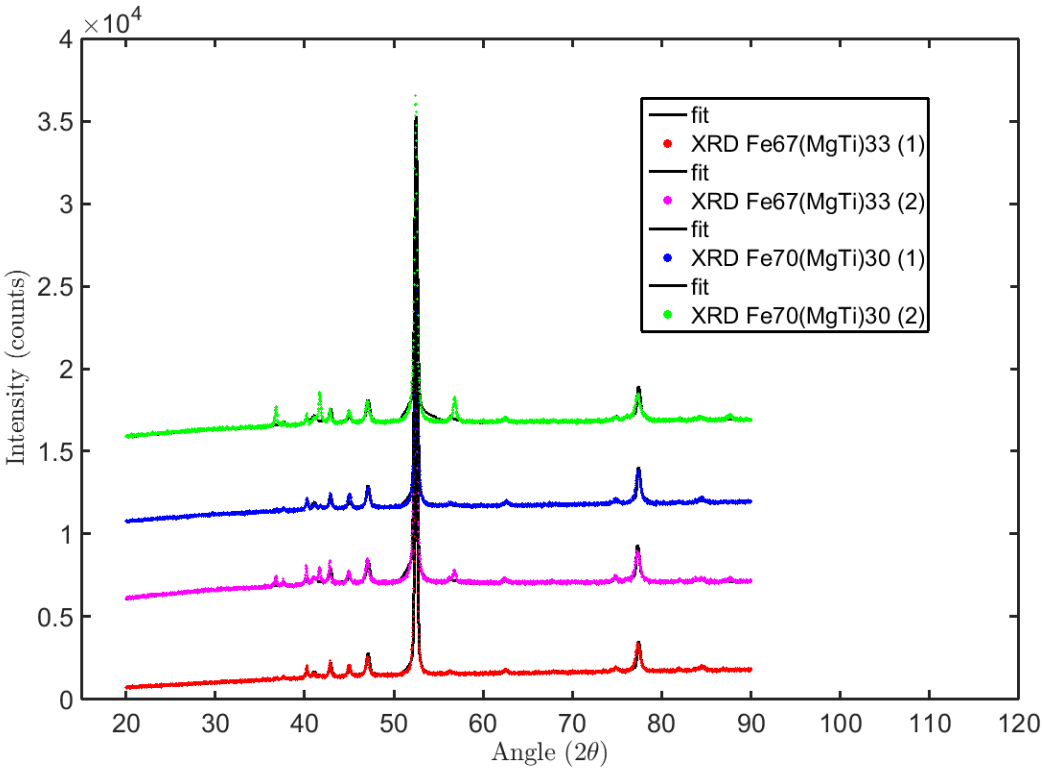


Figure 16: XRD spectrum of Fe-MgTi compounds after 4 hour of high speed ballmilling

| | $Fe_{70}MgNi_{30}$ sample 1 | | | $Fe_{70}MgNi_{30}$ sample 2 | | |
|---|---|---|---|---|---|---|
| | $\chi^2$ | 4.75 | | $\chi^2$ | 15.1 | |
| | fraction % | cell parameters Å | | fraction % | cell parameters Å | |
| phase | | a&b | c | | a&b | c |
| $MgNi_2$ | 0.04 | 4.7614 | 5.199 | 0 | | |
| $MgZn_2$ | 0.8 | 4.787 | 7.806 | 0.83 | 4.788 | 7.7804 |
| $MgCu_2$ | 4.1 | 7.050 | 7.050 | 4.52 | 7.050 | 7.050 |
| a-Fe | 73.5 | 2.862 | 2.862 | 70.88 | 2.862 | 2.867 |
| Mg Occ/24 | 8.58 | 3.202 | 5.199 | 14.32 | 3.202 | 5.199 |
| Ti Occ/24 | 8,9 | 2.946 | 4.674 | 9.46 | 2.946 | 4.674 |

| $Fe_{67}MgTi_{33}$ sample 1 | | | | $Fe_{67}MgTi_{33}$ sample 2 | | |
|---|---|---|---|---|---|---|
| $\chi^2$ | **4.73** | | | $\chi^2$ | **6.99** | |
| | **fraction %** | **cell parameters Å** | | **fraction %** | **cell parameters Å** | |
| **Phase** | | **a&b** | **c** | | **a&b** | **c** |
| $MgNi_2$ | 0 | | | 0,07 | 4.761 | 15.891 |
| $MgZn_2$ | 1.11 | 4.788 | 7.804 | 0 | | |
| $MgCu_2$ | 4.61 | 7.049 | 7.047 | 4,12 | 7.050 | 7.047 |
| a-Fe | 70.02 | 2.862 | 2.862 | 74,11 | 2.869 | 2.869 |
| Mg Occ/24 | 14.61 | 3.201 | 5.199 | 13,07 | 3.202 | 5.199 |
| Ti Occ/24 | 9.65 | 2.945 | 4.674 | 4,12 | 2.946 | 4.674 |

The mixed powder samples were compressed into pellets and sealed in quarts tubes filled with argon to prepare them for heat treatment. The two samples of stoichiometric composition and sample 1 of the non-stoichiometric composition were shortly meltspinned, meaning they were heated to high temperature for a few seconds. This was done hoping that some fusion of the elements would happen without leaving time for the magnesium to evaporate. After 3 weeks of annealing in the oven at 800C the samples were analysed again.

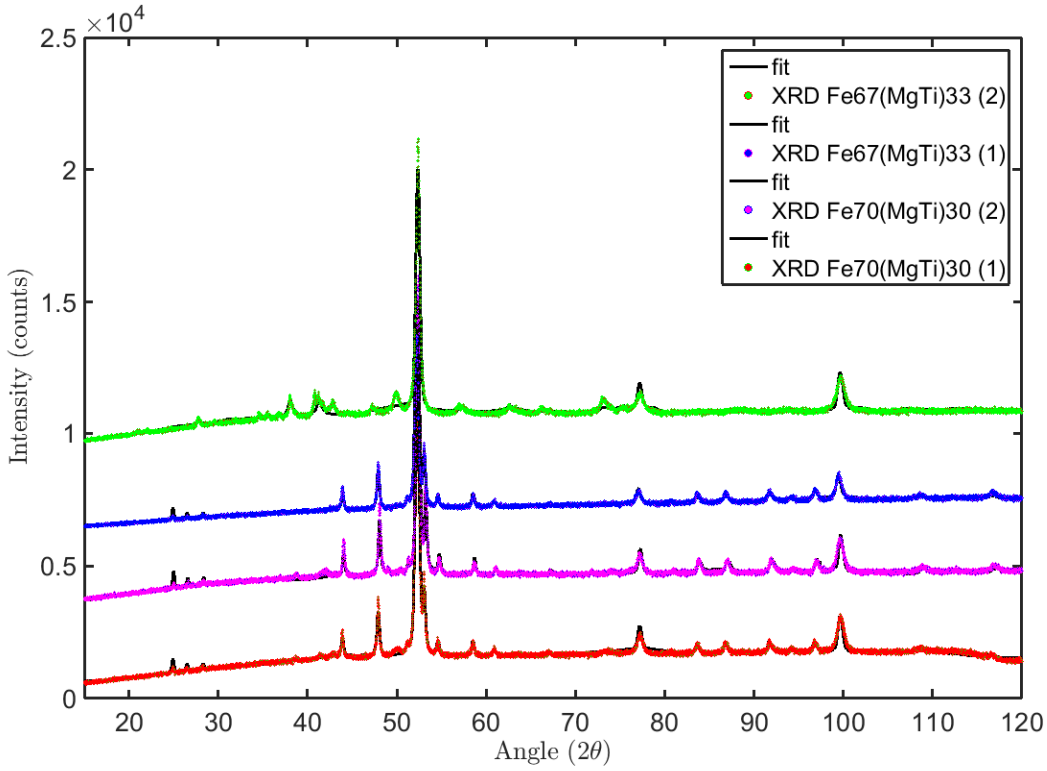


Figure 17: XRD of Fe-MgTi compounds after 3 weeks of annealing

| | $Fe_{70}MgTi_{30}$ sample 1 | | | $Fe_{70}MgTi_{30}$ sample 2 | | |
|---|---|---|---|---|---|---|
| | $\chi^2$ | 4.17 | | $\chi^2$ | 4.55 | |
| | fraction | cell parameters | | fraction | cell parameters | |
| phase | % | a&b [Å] | c [Å] | % | a&b [Å] | c [Å] |
| $MgNi_2$ | 0 | | | 0 | | |
| $MgZn_2$ | 43.17 | 4.788 | 7.806 | 45.6 | 4.774 | 7.784 |
| $MgCu_2$ | 0 | | | 0 | | |
| α-Fe | 56.38 | 2.869 | 2.869 | 54.4 | 2.868 | 2.868 |

| | $Fe_{67}MgTi_{33}$ sample 1 | | | $Fe_{67}MgTi_{33}$ sample 2 | | |
|---|---|---|---|---|---|---|
| | $\chi^2$ = | 2.3 | | $\chi^2$= | 5.98 | |
| | fraction | cell parameters | | fraction | cell parameters | |
| phase | % | a&b [Å] | c [Å] | % | a&b [Å] | c |
| $MgNi_2$ | 0 | | | | | 0 |
| $MgZn_2$ | 51.15 | 4.787 | 7.806 | 30.88 | 4.788 | 7.806 |
| $MgCu_2$ | 0 | | | 0 | | 0 |
| α-Fe | 48.85 | 2.874 | 2.874 | 6.55 | 2.869 | 2.869 |
| Fe2O3 | 0 | | | 5.56 | 5.073 | 14.049 |

All the samples have a very similar crystal structure. Approximately half of the iron has reacted with the titanium to form the $MgZn_2$ structure. The other half is still present as bcc iron. Magnesium has evaporated. It is decided that it would be better to anneal the samples at a temperature slightly under the melting temperature of Mg, which is 650 C.

The magnetocaloric measurements show that the material is ferromagnetic, which is to be expected considering the high fraction of iron. The magnetization is proportional to the amount of iron. The small discontinuity around 300 K can probably be explained by the phase change of $Fe_2Ti$.

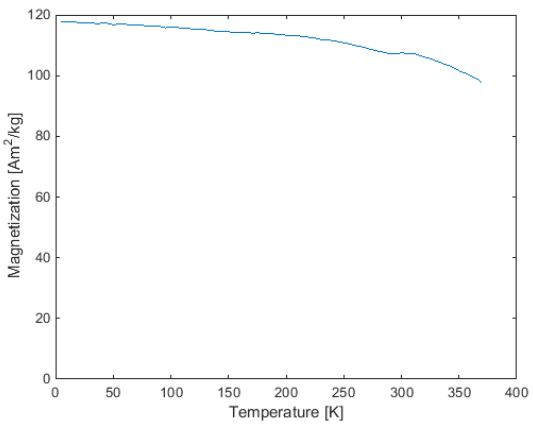


Figure 18: SQUID result of $Fe_{70}MgTi_{30}$ sample 1

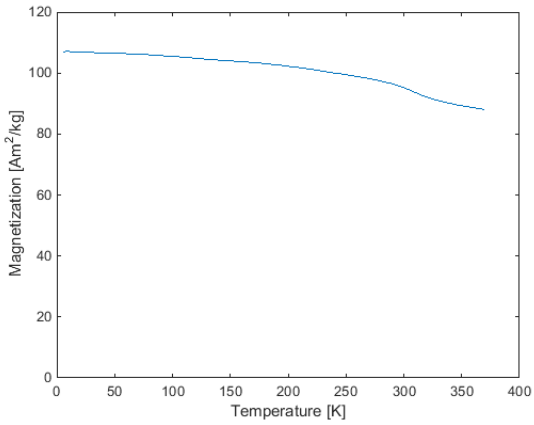


Figure 19: SQUID of $Fe_{70}MgTi_{30}$ sample 2.
All squid measurements are done in a field of 1 T.

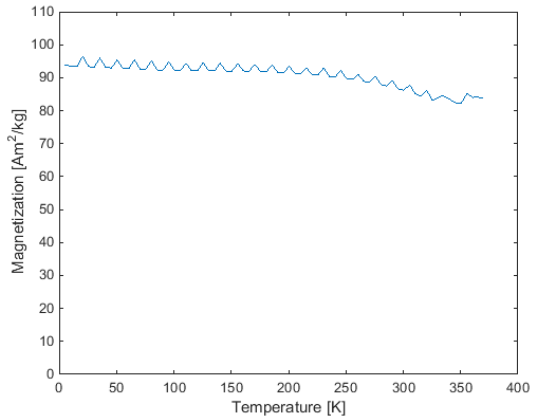


Figure 3: SQUID of $Fe_{67}(MgTi)_{33}$ sample 1

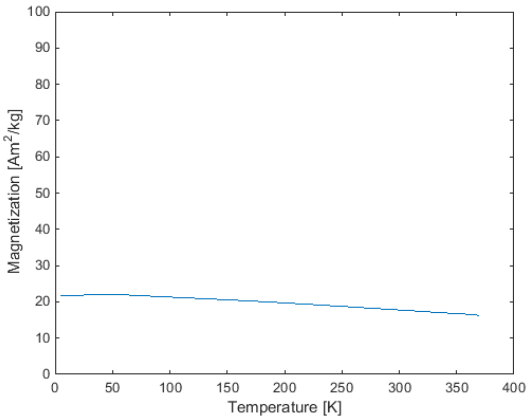


Figure 4: SQUID of $Fe_{67}(MgTi)_{33}$ sample 2

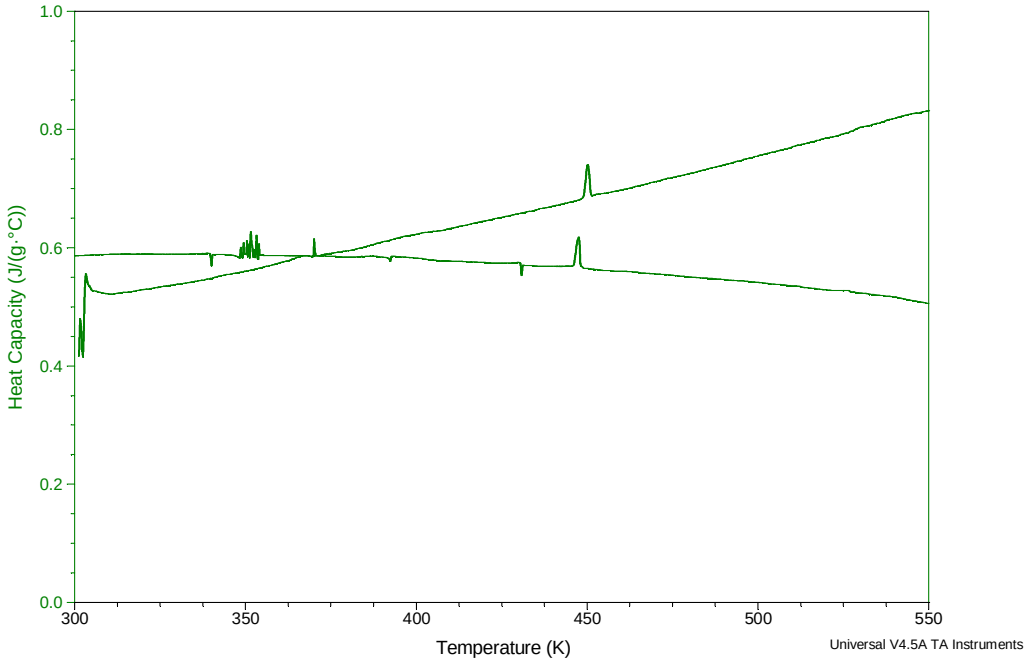


Figure 20: Heat capacity measurement of $Fe_{70}(MgTi)_{30}$ sample 1

In the DSC measurement small peaks in heat capacity are observed at 450 K. Because many graphs produced by this DSC device show small peaks at this temperature, this is probably inherent to the measuring process, and doesn't indicate a magnetic phase transition.

A last attempt to make Fe-MgTi compound is made. This time the samples are annealed for one week at 650°C. The preparation of the samples is now done by drs. M.F.J. Boeije himself. XRD results are clearly different but still not as was hoped for.

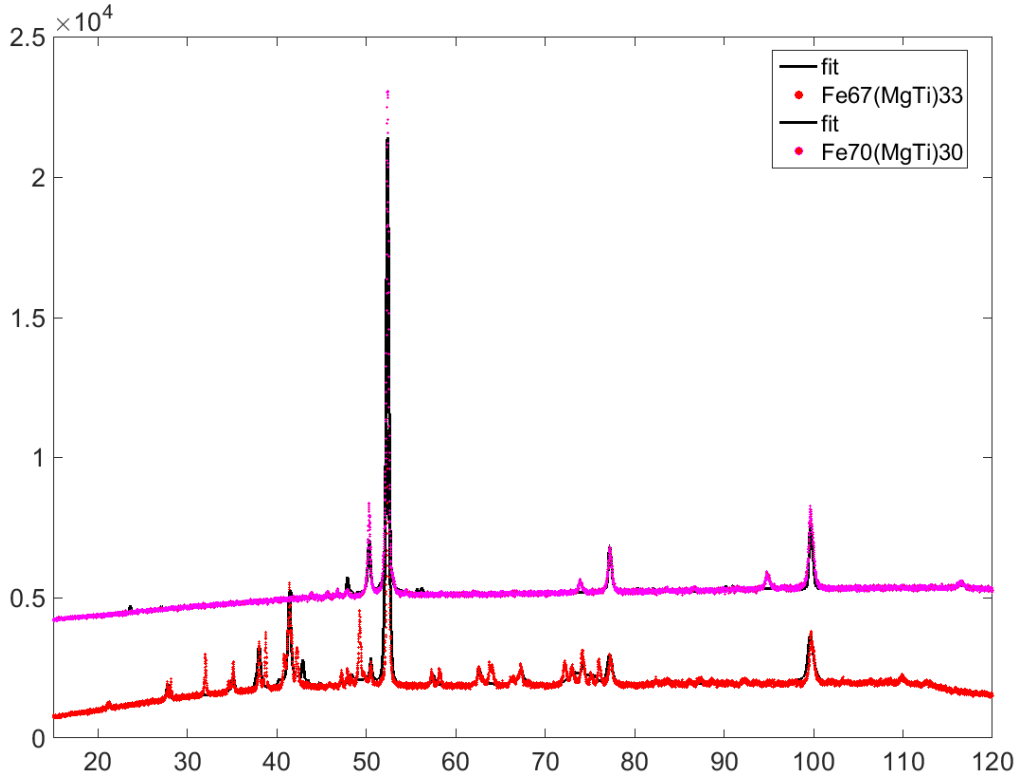


Figure 21: XRD spectrum of Fe-MgTi after 1 week annealing

| $Fe_{70}(MgTi)_{30}$ | | | $\chi^2$=6.2 | | |
|---|---|---|---|---|---|
| | | | fraction | cell parameters | |
| phase | | | % | a&b [Å] | c [Å] |
| $MgNi_2$ | Fe2(MgTi) | P63mmc | 0 | | |
| $MgCu_2$ | Fe2(MgTi) | P63mmc | 0 | 5.050 | 7.658 |
| $MgZn_2$ | Fe2Ti | P63mmc | 1.39 | 6.949 | 6.921 |
| α-Fe rt | Fe,Mg,Ti | Im-3m | 98.31 | 2.868 | 2.868 |
| Cu cF4/225 | Mg | Fm-3m | 0.19 | 4.585 | 4.585 |

| $Fe_{67}(MgTi)_{33}$ | | | $\chi^2$ =30.3 | | |
|---|---|---|---|---|---|
| | | | fraction | cell parameters | |
| phase | | | % | a&b [Å] | c [Å] |
| $MgNi_2$ | | | 0 | | |
| $MgCu_2$ | Fe2(MgTi) | | 0 | | |
| $MgZn_2$ | Fe2Ti | | 0 | | |
| α-Fe rt | Fe,Mg,Ti | Im-3m 229 | 58.61 | 2.869 | 2.869 |
| $Al_2O_3$ | Fe2O3 | R 3c | 7.5 | 5.065 | 14.098 |
| $Fe_3O_4$ | Fe3O4 (Mg) | Fd-3m | 15.22 | 8.394 | 8.394 |
| NiO,hR6,166 | FeO | R -3m | 1.11 | 2.949 | 7.352 |
| Mg 0cc/24 | Mg | P63/MMC | 14.52 | 2.949 | 7.352 |
| Mg occ/24 | Ti | P63/MMC | 2.08 | 2.867 | 4.602 |

Since the amount of $\alpha$-Fe is so big, especially in the $Fe_{70}(MgTi)_{30}$ sample, it can't possibly be only from iron. Mg and Ti can also form this crystal structure type, so it is probable they did. To make this clear, possible elements and space groups have been added in the table. The $Fe_{67}(MgTi)_{33}$ sample was broken, therefore this sample contains several oxides. This also explains why it has a much lower magnetization than the $Fe_{70}(MgTi)_{30}$. The sample shows some irregularity in magnetization, that seem to indicate hysteresis. From the heat capacity measurement nothing special can be concluded, though. It's looks the same as in the previous samples, so no hysteresis occurs.

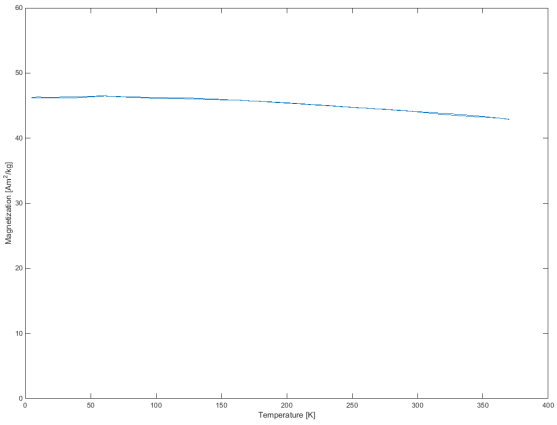


Figure 22: SQUID of $Fe_{67}(MgTi)_{33}$

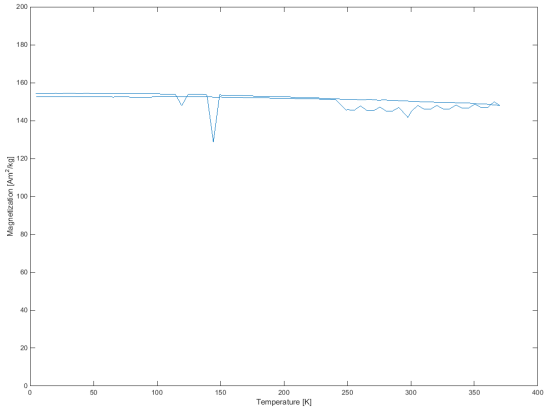


Figure 23: SQUID of $Fe_{70}(MgTi)_{30}$

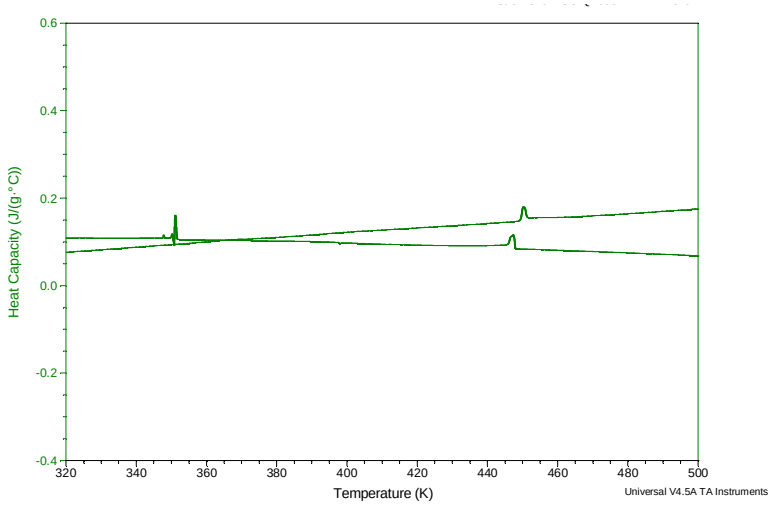


Figure 24: DSC of $Fe_{67}(MgTi)_{30}$

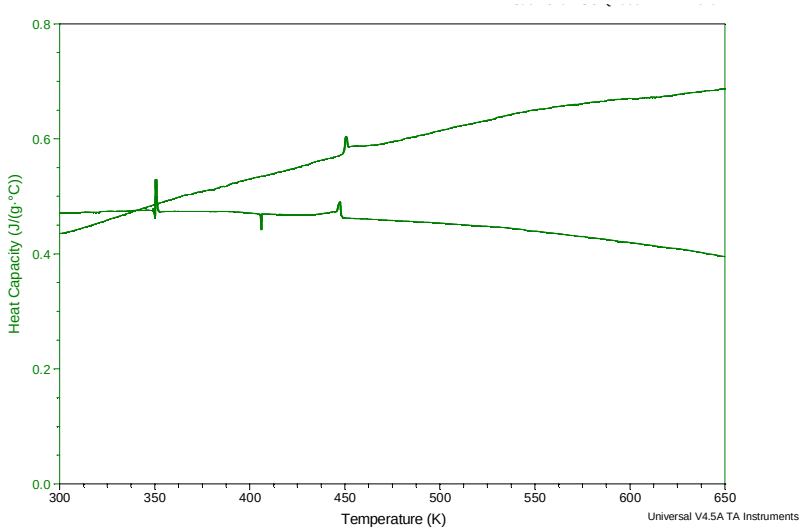


Figure 25: DSC of $Fe_{67}(MgTi)_{30}$

## 3.2-Two Y-FeNi compounds

Two versions FeNiY were prepared, a stoichiometric one with extra FeNi. Based on the article by Christopher at all. [35] it was expected to find the $MgNi_2$ crystal phase, or at least partly. Nonetheless, the $MgNi_2$ phase was not attained. As can be seen from the SQUID measurements, the magnetization of $(FeNi)_{70}Y_{30}$ decreases too gradually to be of any use for magnetic refrigeration. The Curie temperature is only about 150° above room temperature though.

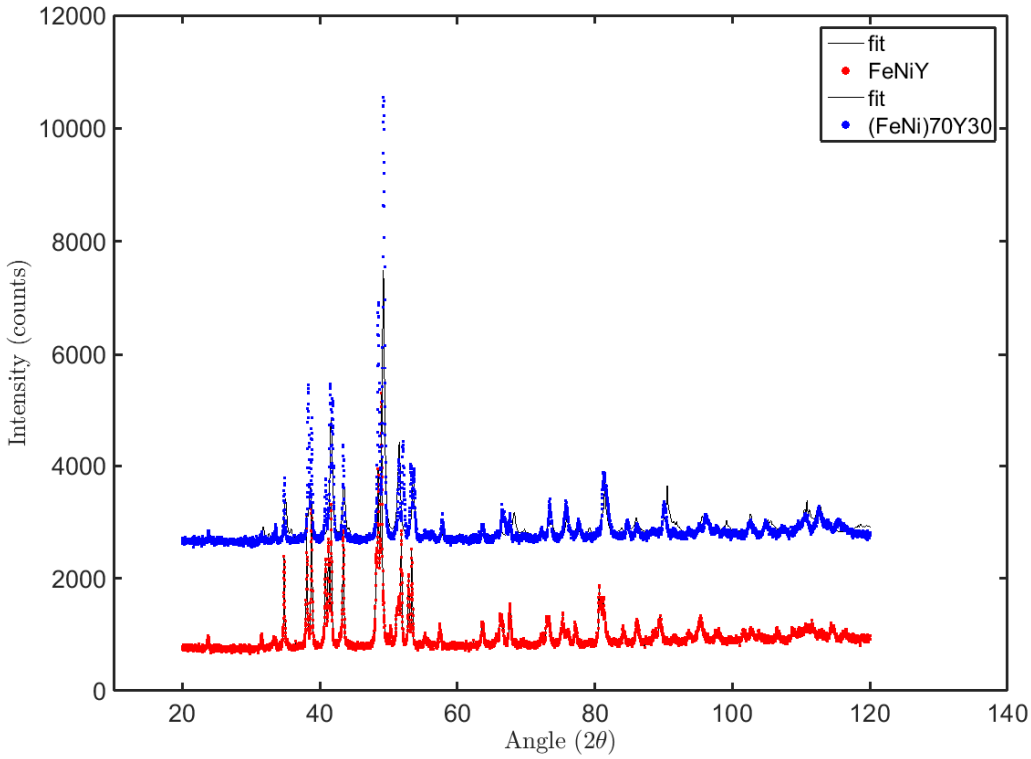


Figure 26: XRD spectrum af Y-FeNi compounds

| **FeNiY** | $\chi^2 = 49.6$ | | | |
|---|---|---|---|---|
| | **fraction** | | **cell parameters** | |
| **phase** | **%** | **a [Å]** | **b [Å]** | **c [Å]** |
| YFeNi ht MgNi2-phase | 0.04 | 7.198 | 7.198 | 7.198 |
| YFeNi rt Cu phase | 0 | | | |
| YNi ht Occ / 48 | 5.78 | 7.139 | 4.106 | 5.506 |
| $Y_{0.95}Ni_2$ and its hydride | 79.04 | 14.326 | 14.326 | 14.326 |
| α-Fe | 15.14 | 2.818 | 2.818 | 2.818 |

| $(FeNi)_{70}Y_{30}$ | | $\chi^2 = 30.81$ | | |
|---|---|---|---|---|
| | **fraction** | **cell parameters** | | |
| **phase** | **%** | **a [Å]** | **b [Å]** | **c [Å]** |
| YFeNi ht MgNi2-phase | 0 | | | |
| YFeNi rt Cu phase | 0 | | | |
| YNi ht Occ / 48 | 37.94 | 7.162 | 4.129 | 5.353 |
| $Y_{0.95}Ni_2$ and its hydride | 5.04 | 14.248 | 14.248 | 14.248 |
| α-Fe | 10.01 | 2.807 | 2.807 | 2.807 |

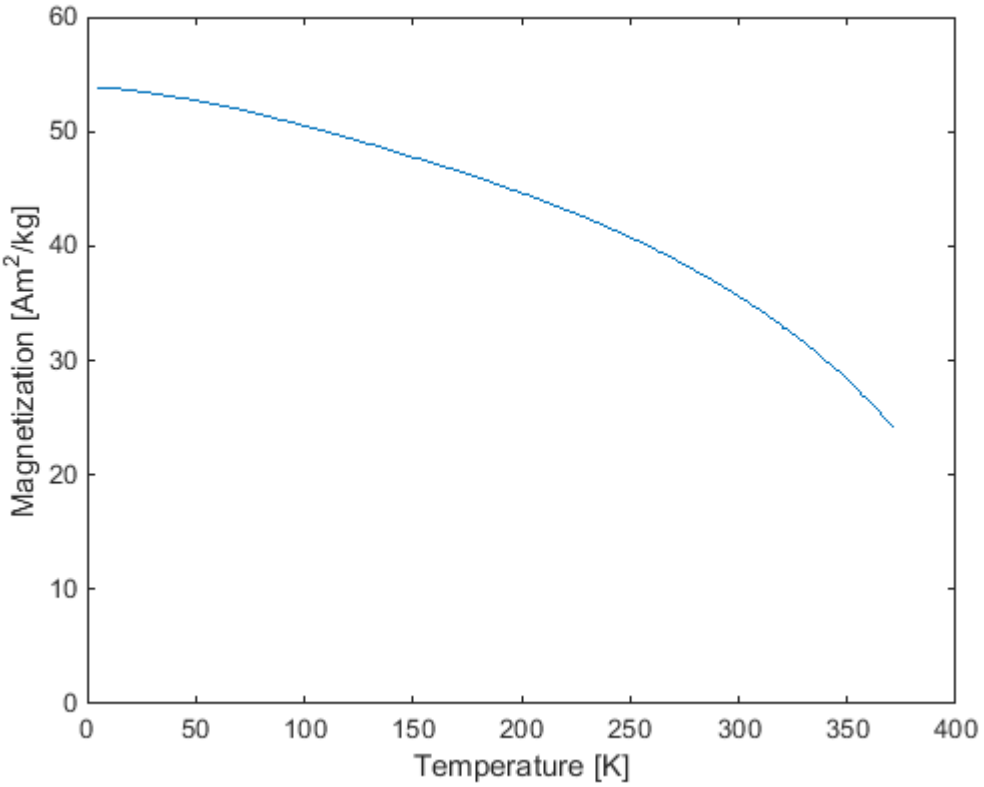


Figure 27: Magnetization-temperature dependance of $(FeNi)_{70}MgTi_{30}$, measured in a field of 1T

## 3.4-Non stoichiomatric compounds of Fe-ZrY

In the article of K. Kai et al. [36] it is reported that Fe-Zr compounds containing between 27.3 to 31.4% of Zirkonium form the $MgNi_2$ phase. A bigger percentage of Zr gives the $MgCu_2$ phase, like is the case with stoichiometric $Fe_2Sc$. $Fe_2Zr$ has a Curie temperature around 600 K. This temperature can be slightly lowered by adding yttrium, as can be seen in the article by Kobayachi and Kanematsu [36], who substituted Zr partly by the Y in the stoichiometric compound. Yttrium also is considerably cheaper than zirkonium. $YFe_2$ has the MgCu2 crystal phase, but the non-stoichiometric compound with excess iron doesn't form a stable phase. Therefore it was decided to investigate the possibility to substitute Zr in the compound with 70% Fe, partly by Y. In the three samples, 25%, 50% and 75% of Zr is substituted by Y.

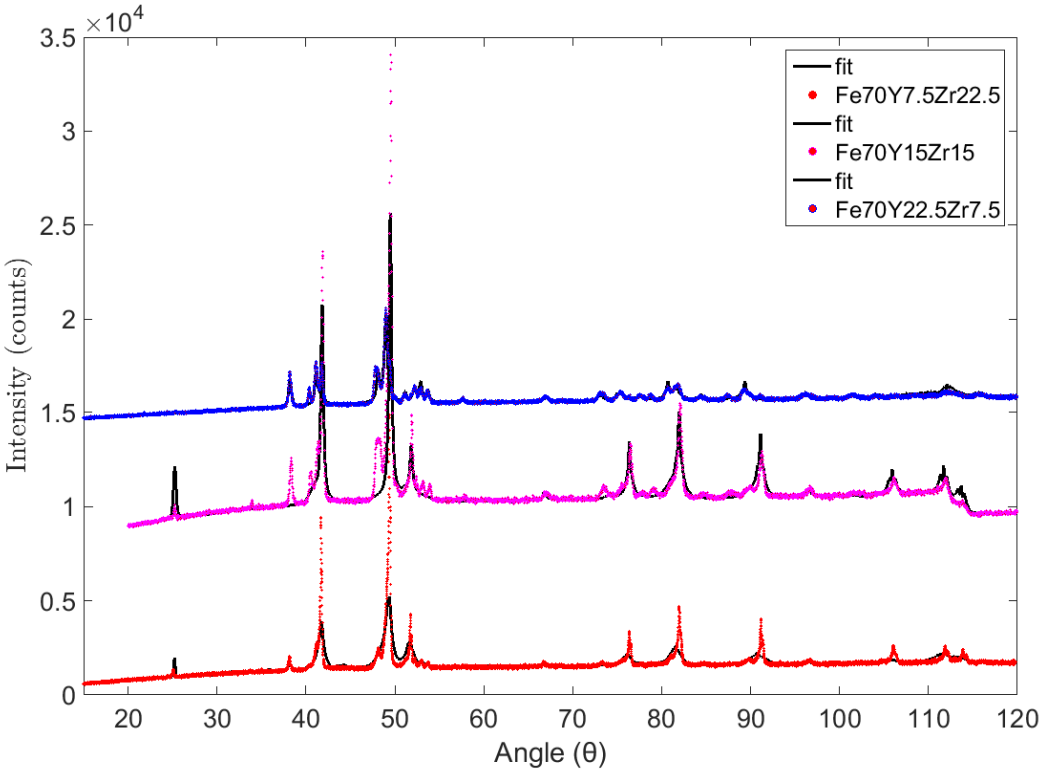


Figure 28: XRD spectra of $Fe_{70}(Y_xZr_{1-x})3$

| | $Fe_{70}Y_{7.5}Zr_{22.5}$ | $\chi^2$=31.8 | |
|---|---|---|---|
| | **fraction** | **cell parameters** | |
| **phase** | **%** | **a&b [Å]** | **c [Å]** |
| $MgNi_2$ | 0 | | |
| $MgCu_2$ | 0 | | |
| $Gd_2Co_7$,hR54,166 | 99.36 | 5.088 | 24.529 |
| $MgCu_4Sn$,cF24,216 | 0.63 | 14.241 | 14.241 |
| | **$Fe_{70}Y_{15}Zr_{15}$** | **$\chi^2$=46.6** | |
| | **fraction** | **cell parameters** | |
| **phase** | **%** | **a&b [Å]** | **c [Å]** |
| $MgNi_2$ | 0 | | |
| $MgCu_2$ | 100 | 7.088 | 7.088 |
| | **Fe70Y22.5Zr7.5** | **$\chi^2$=8.59** | |
| | **fraction** | **cell parameters** | |
| **phase** | **%** | **a&b [Å]** | **c [Å]** |
| $PuNi_3$,hR36,166 | 100 | 5.088 | 24.392 |

The $PuNi_3$ crystal stucture corresponds to $YFe_3$. In the article by Itoh at all. about $Fe_{2.9}$ $Y_{(1-x)}Zr_{(x)}$ compounds is reported on the magnetic properties of this compound. From the large $\chi^2$ values in the Zr rich samples can be deduced that other phases must be present as well, except from the ones that were matched. That makes further measurements on these samples unnecessary.

# 4-Conclusions and recommendations

Not much can be concluded from the analyses of the samples. The hypothesis was that, since $Fe_2Sc$ with the $MgNi_2$ crystal structure has a first-order magnetic transition, there must be other iron compounds with the $MgNi_2$ structure that exhibit this phase change. Two possibilities were examined: a compound with the same number of valence electrons ($Fe_{70}MgTi_{30}$) and iron compounds with a rare earth metal, neighboring scandium in the periodic table ( $(FeNi)_{2-2.1}Y$ and $Fe_{2.1}Y_{(1-x)}Zr_{(x)}$), which were likely to attain this crystalstructure. However, the $MgNi_2$ phase was not found in any of those samples. Therefore this hypothesis cannot be confirmed nor rejected. Also, no promising magnetic behavior in the context of magnetic refrigeration has been encountered in the samples. But to find something new by trial and error during just half a year, would be very improbable.

It appears that achieving the $MgNi_2$ crystal phase is not easy. As a control, a $Fe_{70}Sc_{30}$ sample was made by drs. M. F. J. Boeije, supervisor and initiator of this project. Also the crystal structure of this sample was not purely $MgNi_2$, it contained both the MgNi2 and MgZn2 phase and after annealing the $MgZn_2$ phase dominated. Nevertheless, DSC measurements of this sample show some heat capacity peaks at the around 350°C, which comes pretty close to the transition temperature of 380°C, measured in the article of Pokatilov et al.

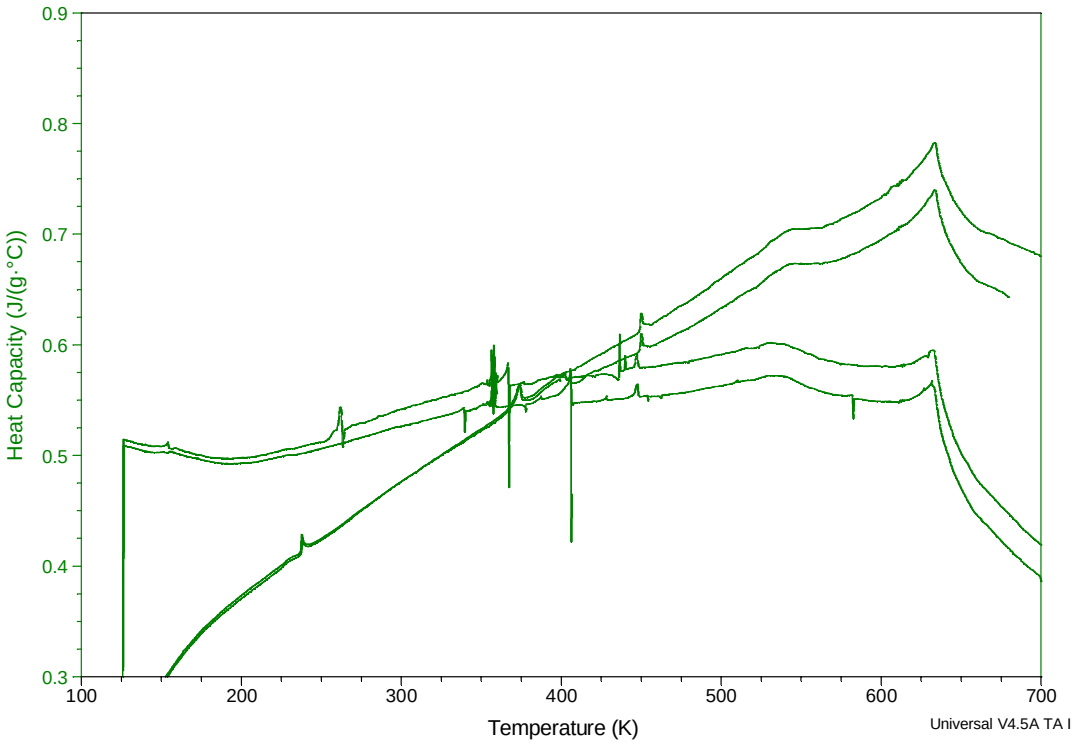


**Figure 29: Heat capacity measurement of a $Fe_2Sc$ sample**

It would be interesting to see what kind of transition these peaks indicate. Therefore, it is necessary to measure the magnetization temperature dependence at high temperatures, which can not be done at the TU Delft. Even if this compound doesn't have $MgNi_2$ phase, but the $MgZn_2$ phase instead, it would be interesing to measure the magnetic behavior. The first-order phase transition of $Fe_2Hf_{(1-x)}Ta_{(x)}$ reported on in [20] is similar to that of $Fe_2Sc$, while this compound has the $MgZn_2$ structure. Extra proof for a first-order phase transition in $MgZn_2$ crystal type materials would be valuable, since this crystal structure is easier to attain, for instance with compounds containing titanium.

Pokatilov et al. concluded that the phase transition of the Fe-Sc compound with the $MgNi_2$ structure is a ferro- antiferromagnetic one. The type of magnetism above 380°C wasn't measured by them though. It would be interesting to validate experimentally if this conclusion is true, if $Fe_{2.05}Sc_{0.95}$ indeed becomes antiferromagnetic at this temperature or just paramagnetic. This can be done by determining the susceptibility above the transition temperature, by measuring the magnetization while varying the B-field.

To continue making $Fe_2MgTi$ compounds, I would certainly not recommend, as the list of failed attempts in doing this illustrates. It is still plausible that there are more $MgNi_2$ compounds with a first-order transition, not many of them have been investigated, and the few samples presented in this thesis should not be a demotivating factor in looking for others. However, it is necessary to first replicate the results of the Fe-Sc compound with $MgNi_2$ phase, since this is the only compound known with this crystal structure that has a first-order magnetic transition. Only when those results are confirmed it is justified to put more effort in looking for similar compounds.

# References


[1] B. Yu, M. Liu, P.W. Egolf, A. Kitanovski, *A review of magnetic refrigerator and heat pump prototypes built before the year 2010,* Int. J. Refrig. Vol. 33, p.1029 (2010).

[2] V.K. Pecharsky, K.A. Gschneidner Jr., *Giant magnetocaloric effect in $Gd_5(Si_2Ge_2)$,* Phys. Rev. Lett, Vol. 78 (23) p. 4494–4497 (1997).

[3] O. Tegus, E. Brück, K. H. J. Buschow, F. R. de Boer, *Transition-metal-based magnetic refrigerants for room-temperature applications* Amsterdam: Van der Waals Zeeman Instituut, Nature, Vol. 415, p. 150-152 (2002).

[4] N. H. Dung, L. Zhang, Z. Q. Ou, E. H. Brück *Magneto-elastic coupling and magnetocaloric effect in hexagonal Mn-Fe-P-Si compounds,* Delft: Fundamental Aspects of Materals and Engery (FAME) arXiv:1205.6196 [cond-mat.mtrl-sci] (2012).

[5] *Premiere of cutting-edge magnetocaloric cooling appliance,* BASF. (2015) retrieved from: http://www.basf-new-business.com/en/projects/e-power-management/solid-state-cooling/.

[6] V.S. Pokatilov, V.V. Sadchikov, Y.F. Sidokhin, O.V. Utenkova, *Structure and magnetic properties of Fe-Sc alloys,* Moscow: M.V. Lomonosov State University, Fiz. Met. Metalloved. Vol. 62, p. 69-75, (1986)

[7] A. Smith, *Who discovered the magnetocaloric effect*, Eur. Phys. J. H 38, p. 507 (2013).

[8] A. M. Tishin, Y. I. Spichkin, *The magnetocaloric effect and its applications,* Bristol: institute of physics publishing (2003).

[9] H. Yibole, *Nature of the first-order magnetic phase transition in giant-magnetocaloric materials,* Thesis TU Delft (2015).

[10] P.D. Olmsted, *Lectures on Landau Theory of Phase Transitions*, University of Leeds, Department of Physics and Astronomy (2000).

[11] A. Aharoni, *Introduction to the Theory of Ferromagnetism,* Oxford university press (2000).

[12] Kurt Binder, *Theory of first-order phase transitions*, Rep. Prog. Phys. Vol. 50, (7) , p.783-859 (1987).

[13] Lecture from University of California Davis, retrieved from: http://yclept.ucdavis.edu/course/240C/Notes/Landau/LandauPhaseTrans.pdf

[14] M. Niemeyer et al., *Spin Coupling and Orbital Angular Momentum Quenching in Free Iron Clusters,* Phys. Rev. Lett. Vol. 108, 057201 (2012).

[15] D.J. Griffiths, *Introduction to Quantum Mechanics*, 2nd edition,p Pearson education limited, p. 211. (2014).

[16] M. Manekar, S. B. Roy, *Reproducible room temperature giant magnetocaloric effect in Fe–Rh,* J.Phys. D: Applied Physics, Vol. 41, (19), (2008).

[17] *http://mineralprices.com/*

[18] D. W. Forester, *Amorphous $YFe_2$—A concentrated spin glass,* J. Appl. Phys. Vol. 50, p. 7336 (1979).

[19] C. Kittel, *Model of Exchange-Inversion Magnetization,* Phys. Rev. Vol. 120 (2), p. 335 (1960).

[20] Y. Nishihara, Y. Yamaguchi, *Magnetic phase transitions in Itinerant electron magnets,* Phys. Soc. Japan, Vol. 23, p 935-938, (1983).

[21] T. Moriya, K. Usami, coexistence of ferro- antiferromagnetic and phase transitions in itinerant electron systems, Solid State Comm., Vol. 23, p. 935-938. (1970).

[22] G. H. Wertheim, D.E.N. Buchanan, J. H. Wernick, *Magnetic Properties of Inequivalent Iron Atoms in Fe2Ti*, Solid State Comm., Vol. 8, p. 24, (1970).

[23] K. Adachi, *3d, 4d and 5d Elements, Alloys and Compounds*, chapter *1.2.3 Alloys of Fe, Co or Ni and Ti, V, Cr or Mn,* Vol. 19a of the series Landolt-Börnstein - Group III Condensed Matter p. 316-322 (1986)

[24] J.Pelloth, R.A. Brand, W. Keune, *Local magnetic properties of the Fe2Ti laves phase,* J. of Magn. Magn. Mat. Vol. 140-144 p.15-60 (1995).

[25] Y. Wu, X. Wu, S. Qin, K. Yang, *Compressibility and phase transition of intermetallic compound $Fe_2Ti$,* J. Alloys Comp. Vol. 558, p. 160–1635 (2013).

[26] J.M.D. Coey, *Magnetism and Magnetic Materials*, Cambridge University Press (2010).

[27] ChemWiki: The Dynamic Chemistry Hypertext > Textbook Maps > Inorganic Chemistry Textbook Maps > Map: Inorganic Chemistry (Wikibook) > Chapter 6: Metals and Alloys - Structure, Bonding, Electronic and Magnetic Properties > 6.3: Crystal structures of metals

[28] https://en.wikipedia.org/wiki/Allotropes_of_iron

[29] J.R. Hook, H. E. Hall, *Solid state physics,* 2nd edition, Department of Physics University of Manchester (1974).

[30] ChemWiki: The Dynamic Chemistry Hypertext > Textbook Maps > Inorganic Chemistry Textbook Maps > Map: Inorganic Chemistry (Wikibook) > Chapter 6: Metals and Alloys - Structure, Bonding, Electronic and Magnetic Properties > 6.7: Ferro-, ferri- and antiferromagnetism

[31] http://magician.ucsd.edu/essentials/WebBookse18.html

[32] M.F.J. Boeije et al, *Efficient Roomtemperature Cooling with Magnets*, Chem. mater. (2016).

[33] M. Getzlaff, *Fundamentals of Magnetism,* Springer-Verlag Berlin Heidelberg (2008).

[34] S. Rousselot, M. P. Bichat, D. Guay, L. Roué, *Structure and electrochemical behaviour of metastable$Mg_{50}Ti_{50}$ alloy prepared by ball milling,* J. Power Sources 175, p. 621-624, (2008).

[35] J.T. Christopher, A.R. Piercy, K.N.R. Taylor, *The lattice parameters of various series of pseudo-binary rare-earth-transition metal laves phase compounds,* J. the Less Comm. Met., Vol 17 (1), p. 59-63 January (1969),.

[36] K. Kai, T. Nakamichi, M Yamakoto, *Crystal structures and magnetic properties of intermetallic Fe2Zr*, Tôhoku University, Sendai (1968).

[37] K. Kobayashi, K. Kanematsu, *Magnetic Properties and Crystal Structure of Laves Phase ($Y_xZr_{1-x}$)$Fe_2$ and Their Hydrides,* J. Of Phys. Soc. Jpn, Vol. 55 (1986), 1336-1340

[38] K. Itoh, T. Okagaki, K. Kanematsu, *Crystal Structure and Magnetic Properties of $Y_{1-x}Zr_xFe_{2.9}$,* J. Phys. Soc. Jpn. Vol. 58, p. 1787-1792 (1989)

# Appendix A

## Structure and Magnetic Properties of Fe-Sc Alloys

**B. C. Pokatilov, V.V. Sadchikov, E.F. Sidohin, O.V. Utenkova**

Translation by F. J. le Roy

The crystal structure of Fe-Sc alloys containing 0,25-33,3 at.% Scandium was defined by the methods : nuclear magnetic resonance (NMR) in the nuclei of 45Sc and 57Fe and radiography. The joint analysis of these methods has shown the structure of alloys that contain alpha-Fe and $Fe_2Sc$, and because of stoichiometry the crystal structure of the $Fe_2Sc$ alloy is of the cubic type $MgCu_2$, and the alloy with a nonstoichiometric composition is a hexagonal $MgNi_2$ type. To define is the ultrafine field on nuclei 45Sc and 57Fe, as well as local magnetic moments of the iron atoms. The magnetization ($\sigma$) of the alloys is measured in a field of 9 kOe in the temperature range 20-900°C. The Curie temperature for $Fe_2Sc$ with crystal structures $MgCu_2$ and $MgNi_2$ is 380+-5° C. For the $Fe_2Sc$ alloy of the $MgNi_2$ structure, hysteresis in the temperature dependence ($\sigma$(T)) is measured. It is assumed that this hysteresis is caused by a magnetic phase transition.

Recently, alloys containing iron with rare earth metals, eg. Fe-Y, Fe-Gd, Fe-Tb and others, have attracted the great interest of scientist. There are a lot of data on the various properties of these alloys. On the contrary literature contains little information on the properties and structure of iron alloys with scandium. In [1] is reported that Fe-Sc alloys contain two intermetallic compounds: $Fe_2Sc$ and $FeSc_3$, and that, in alloys containing about 0-33.3 at. % of Sc, exist the phases $Fe_2Sc$ and $\alpha$-Fe, and in alloys with 33,3-75,0 at.% Sc the phases $Fe_2Sc$ and $FeSc_3$ are found.

The literature contains contradictory information about the Laves phase structure $Fe_2Sc$. In [2] is reported that the compound $Fe_2Sc$ has the $MgNi_2$ (hexagonal)crystal structure, with the parameters a=4,972 Angstrom and c is 16,278 Angstrom. According to [3], there is a $Fe_2Sc$ compound with the $MgCu_2$ type (cubic) crystal structure, with lattice parameters a=7,09 Angstrom. In [4] is detected that the $Fe_2Sc$ compound has the crystal structure $MgZn_2$ (hexagonal), and that the lattice parameters of this structure are a=4.9370 A and c=8,0382 A. These data show that with just röntgen graphic (XRD) methods it is difficult to clearly define the structure of the intermetallic Fe2Sc compounds.

In [4, 5] is reported on some magnetic properties of the $Fe_2Sc$ compound. According to [4], the magnetization of $Fe_2Sc$, measured in a field of 10.5 kOe at 4,2 Kelvin, is ~77emu/g, the average magnetic moment of the iron atom is $\mu$ Fe=1.37 $\mu$ B, and the Curie temperature is Tc=270 ° C. Similar

parameters for $Fe_2Sc$ were measured in [5], they appeared to be Tc=360+- 10 ° C, and the magnetization in a field of 9 kOe at 20° C equals ~77emu/g.

Accordingly, the little studied structural and magnetic properties of the Fe-Sc alloys have a contradictory character. The purpose of this work is to investigate the structure and some magnetic properties of Fe-Sc alloys in the range of compositions containing 0-33 at.% Sc.

Iron-scandium alloys, containing Fe-0,25 at % Sc, Fe-0.10 Sc, Fe-20 Sc, Fe-25 Sc, as well as the alloys close to stoichiometric composition, $Fe_{2.05}Sc_{0.95}$, $Fe_{2.01}Sc_{0.99}$ and $Fe_2Sc$, were arc melted safely in helium atmosphere. The ingots were annealed at 950° C for 30 h and slowly cooled in the oven to room temperature. The structure of the alloys was investigated by the röntgen method using FeK$\alpha$ and CrK$\alpha$ radiation and by the method of magnetic resonance (NMR) in the nuclei 45Sc and 57Fe. For these methods powder samples were used, obtained from the annealed ingots. The crystal structure measurements were conducted at room temperature as well as in the range 20-600° C.
For the alloy $Fe_{2.05}Sc_{0.95}$ the NNMR spectra in the frequency range 20-150MHz were measured at 4.2 K. The magnetization of the alloys was defined with a vibrating magnetometer in a field of 9kOe and in the temperature range 20-900° C. The Curie temperature of the alloys is estimated by the jump of the magnetization when the sample is cooled from a high temperature in an external magnetic field ~ 20 Oe.

## The results of the experiment

Fig. 1 shows NMR spectra of the 45Sc nuclei in the alloys $Fe_2Sc$, $Fe_{2.01}Sc_{0.99}$ and $Fe_{2.05}Sc_{0.95}$. The figure shows that the spectrum of the $Fe_2Sc$ compound contains a narrow single line at 104+-0,0MHz. The hyperfine field around the 45Sc nuclei in Fe2Sc is H0=-100,8kOe.
The sign of the hyperfine field is determined by the shift of the NMR frequency of 45Sc in the external magnetic field.
At the low frequencies in the NMR spectrum satellite lines are observed, therefore the scandium or iron atoms occupy “foreign” sites. The single narrow line in the NMR of 45Sc in Fe2Sc shows that the scandium atom occupies a crystallographic state in the $Fe_2Sc$ lattice.

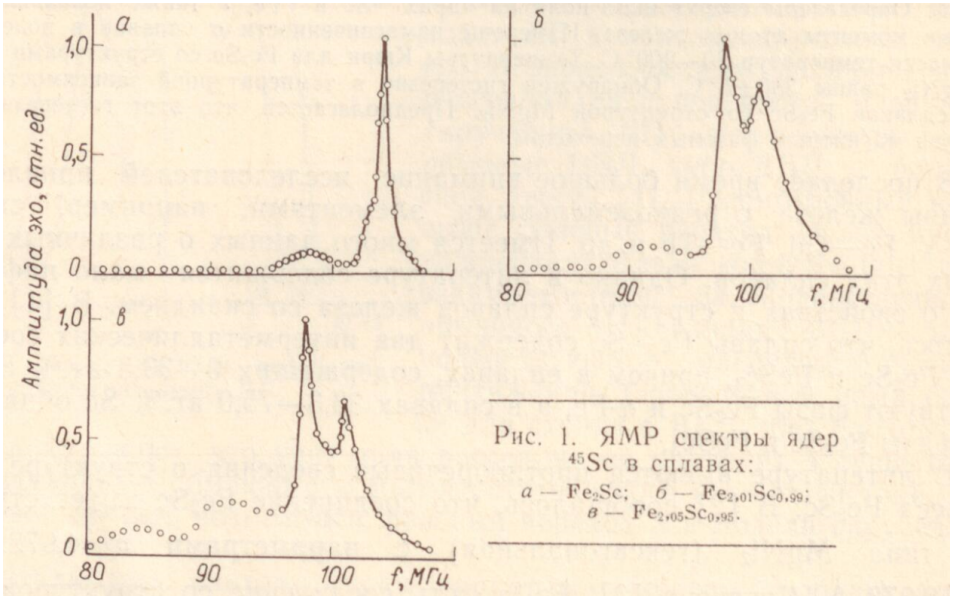


Рис. 1. ЯМР спектры ядер $^{45}Sc$ в сплавах:
а — $Fe_2Sc$; б — $Fe_{2,01}Sc_{0,99}$;
в — $Fe_{2,05}Sc_{0,95}$.

The NMR spectrum of 45Sc in the alloys $Fe_{2.01}Sc_{0.99}$ and $Fe_{2.05}Sc_{0.95}$ (See Figure 1b en c) contains 2 allowed lines with heights at 982+-0.1 and 101.4+-0.1 MHz. This indicates that there are lines which aren't equivalent to the crystallographic state of the scandium atoms in the lattice of the considered alloy. The hyperfine field of 45Sc for these states is 95.0 and 98.1 kOe.

From the NMR spectra can also be seen that with decreasing scandium content in the alloy (less than 33.3 at. %) the intensity of the satellite lines at 90-92 MHz increases. For the alloys Fe-25%Sc and Fe-20%Sc the NMR spectra of 45Sc consist of two Shipok peaks with maxima at 90-92 and 83-85 MHz. This structure of the NMR spectra of the alloys may be due to the fact that for the alloys deviating from the stoichiometric $Fe_2Sc$, a fraction of the iron and scandium atoms occupies different sites in the lattice, causing the increase in intensity of those lines; these alloys, $Fe_{2.01}Sc_{0.99}$ and $Fe_{2.05}Sc_{0.95}$, which are close to stoichiometric composition, cause the satellite lines. In the alloys containing 0.25 , 10 and 25 % of Sc are, besides the above mentioned NMR lines of the 45Sc nuclei, lines observed at 139,5 and 46,7 MHz. The intensity of these lines increases with decreasing scandium content in the alloys. We associate the peak at 139.5 MHz with the NMR of 45Sc ($|H_0|$ =134,9 kOe) in $\alpha$-Fe, and the peak at 46.7 MHz with 57Fe in $\alpha$-Fe, in accordance with the data [6]. Accordingly, the NMR measurements of the Fe-Sc alloys show that 1) The scandium atoms in the $Fe_2Sc$ alloy are in the same crystallographic state as they are in the alloys $Fe_{2.01}Sc_{0.99}$ and $Fe_{2.05}Sc_{0.95}$: in two crystallographically nonequivalent states. 2) The alloys Fe-10, Fe-20 and Fe-25%Sc are biphasic, one of the phases is $\alpha$-Fe, and the other is $Fe_2Sc$, in accordance with the data [1].

Fig . 2 shows the NMR spectra of the 57Fe nuclei in the alloys and $Fe_2Sc$ $Fe_{2.01}Sc_{0.99}$. It can be seen that the NMR spectrum of 57Fe in Fe2Sc has two allowed peaks with maxima at 26,10 ± 0,05 and 27,60 MHz ± 0,05 MHz. The ratio of the areas of those peaks is 1:3.The NMR spectrum of 57Fe in the alloy $Fe_{2.01}Sc_{0.99}$ contains 3 allowed peaks with maxima at 24.0 26.0 and 27 MHz and the ratio of the areas of these peaks is 1:0.7:1. The NMR spectra of 57Fe in the alloys $Fe_{2.01}Sc_{0.99}$ and $Fe_{2.05}Sc_{0.95}$ indicate that in the lattice of this alloy are three different iron atoms in three different states, on contrary, Fe2Sc only has one or two iron states.

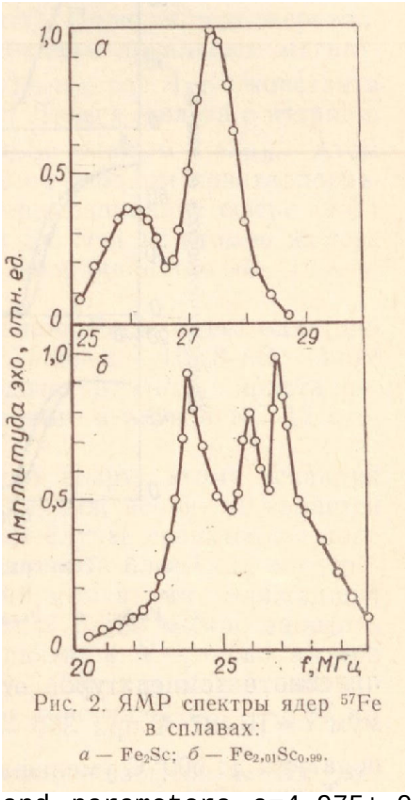

Рис. 2. ЯМР спектры ядер $^{57}Fe$ в сплавах:
$а$ — $Fe_2Sc$; $б$ — $Fe_{2,01}Sc_{0,99}$.

XRD analyses of the alloys $Fe_2Sc$, $Fe_{2.01}Sc_{0.99}$ and $Fe_{2.05}Sc_{0.95}$ and others, containing a higher amount of iron, is based on the data [2-4] and our NMR data of the nuclei 45Sc and 57Fe. The joint analyses of these data shows that the XRD sprectrum of the $Fe_2Sc$ alloy is best described by the structure type $MgCu_2$, since it has a cubic lattice and lenght a=7.05+0.1 Angstrom; however, the alloys $Fe_{2.01}Sc_{0.99}$ and $Fe_{2.05}Sc_{0.95}$ have the MgNi2 cristalstructure, with a hexagonal lattice and parameters a=4.975+-0.002 Å and c=16.318+-0.004 Å. The alloys Fe-25, Fe-20 , Fe- 10 at.%Sc contained $\alpha$-Fe and $Fe_2Sc$ with the $MgNi_2$ type cristal structure. Compounds of the type $Fe_3Sc$, $Fe_{26}Sc_6$ and $Fe_{17}Sc_2$ have not been

found in the samples with this heat treatment, neither with XRD nor with NMR.

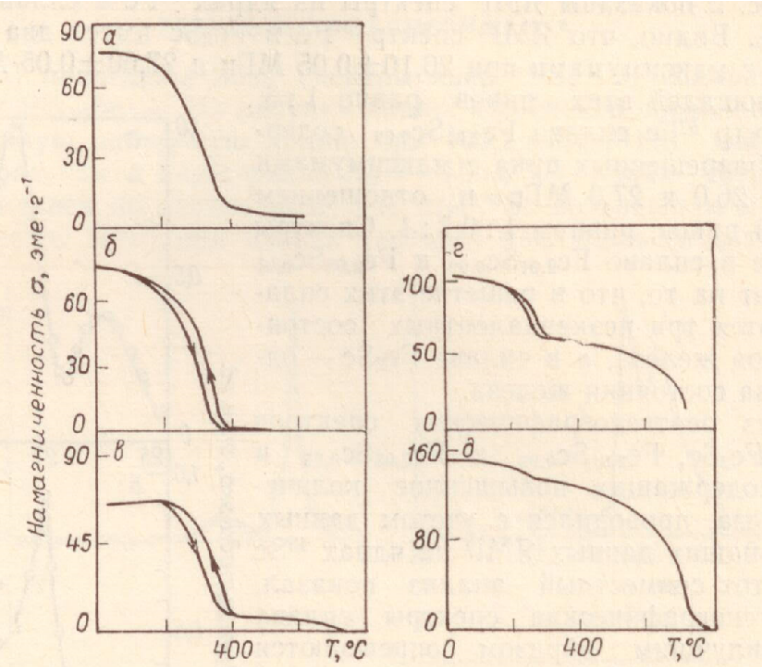


Рис. 3. Температурные зависимости намагниченности в поле 9 кЭ для сплавов:
а — $Fe_3Sc$; б — $Fe_{2,05}Sc_{0,95}$; в — Fe—25 ат.% Sc; г — Fe—20 Sc; д — Fe—10 Sc.

The magnetization of the Fe-Sc alloys as a function of temperature, σ(T), is investigatd and listed in figure 3. It can be seen that the magnetization of the compounds $Fe_2Sc$ with a $MgCu_2$ and a $MgNi_2$ structure is almost the same at 20° C, it is ~77emu/gr. The magnetic transition temperature (the Curie temperature) of these compounds is defined by the jump of the magnetization σ(T) at 380+- 5° C , while cooling from high temperature in a field of 20 Oe. However, on the σ(T) curve of the the alloy $Fe_2Sc$ with a the $MgNi_2$ structure, other abnormalities were observed at ~270 and ~160 ° C. It was also found that the magnetization curve σ(T) of the alloys $Fe_{2.01}Sc_{0.99}$; $Fe_{2.05}Sc_{0.95}$; Fe-25 and Fe-20 at% Sc has hysteresis during heating and cooling, the temperature interval of this coincides with the temperature of the observed abnormalities in σ(T) in the field of 20 Oe. With increasing iron content the Curie temperature of the Fe-Sc alloys in $Fe_2Sc$ phase decreased. In figure 3 can be seen thet the σ(T) curve of the alloys differing in composition from the stoichiometric compound $Fe_2Sc$, consist of curves that correspond to the σ(T) of the phases α-Fe and $Fe_2Sc$. The discussed data on the temperature dependence of the magnetization confirms the conclusions of [1] and our own data that Fe–Sc compounds, containing up to 33% scandium, just exist in the α-Fe and $Fe_2Sc$ phase.

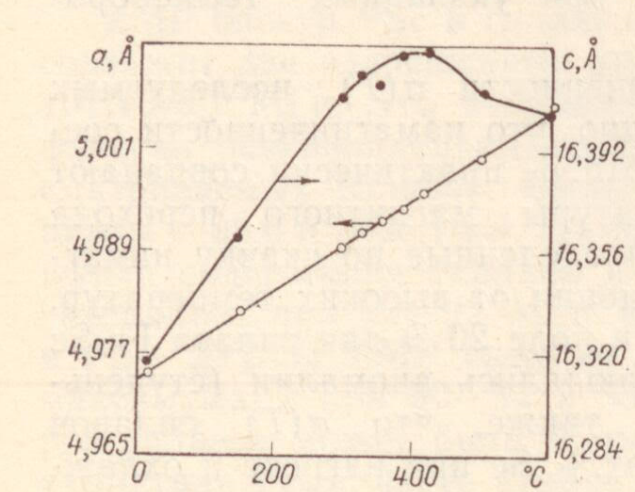


Рис. 4. Температурные зависимости параметров решетки $a$ (○) и $c$ (●) сплава $Fe_{2,05}Sc_{0,95}$.

Figure 4 shows the temperature dependence of the parameters a and c in the hexagonal $MgNi_2$ lattice of the alloy $Fe_{2.05}Sc_{0.95}$ in the temperature interval 20-600 ° C. In can be seen that the lattice parameter a increases linearly with temperature from 4.974 up to 5.005 Å, whereas parameter c at the first increases linearly with temperature up till c=16,320 Å, than reaches a maximum at c=16.427 Å at 360-380 ° C and with a further increase in temperature to 600 ° C is reduced to c = 16.405 Å.

Thus, NMR, XRD and magnetic studies of the alloys Fe-33 at. %Sc show that the stoichiometric composed $Fe_2Sc$ alloy has the crystal structure of the prototype $MgCu_2$, but the alloys containing more iron atoms consist of α-Fe and $Fe_2Sc$ with crystal structure $MgNi_2$. Apparently, the compound $Fe_2Sc$ with $MgCu_2$ structure only exist in a narrow range of concentrations. We assume that the Laves phase with the hexagonal crystal structure of $MgZn_2$, on which is reported in [4], only exist in the compounds containing more than 34 at% scandium.

## Discussion of the results

The iron atoms in the $MgCu_2$ lattice are crystallographically equivalent to one state, and the NMR of the 57Fe nuclei must contain one resonance peak. However, the NMR spectrum, of 57Fe contains two allowed lines with maxima at 26.1 and 27.4 MHz (figure 2a) The ratio of the intensities of those peaks is 1:3. A similar situation is observed for the NMR of 57Fe in $Fe_2Y$ and $Fe_2Zr$, which also have the $MgCu_2$ phase [8,9]. This type of NMR spectrum of 57Fe is due to the fact that the iron atoms in the alloy of the $Fe_2Sc$ ($MgCu_2$) alloy have two magnetically different states, because the easy magnetization axis lies along the < 111 > direction. Then, in accordance with various bipolar contributions in the hyperfine field of 57Fe, the NMR spectrum will be split into two lines with an intensity, which should relate to each other as 1 : 3, which is observed experimentally.

The average hyperfine field of the 57Fe nuclei in Fe2Sc at 4,2 K is 197,6 kOe (taking into account the Lorentz field of ~1,7 kOe). Assuming that the hyperfine field of the 57Fe nuclei in $Fe_2Sc$, associated with the average local magnetic momentum, $\mu_{Fe}$, is related to Ho as $H_0 = A_{Fe}\mu_{Fe}$, where $A_{Fe}$ is the coupling constant, which is 140kOe/μB for Laves type compounds of iron and yttrium [10], we determined that the magnetic moment of Fe in $Fe_2Sc$ is

1,43 μB. An iron atom in $Fe_2Sc$ is in a single crystallographic state and is surrounded in the first coordination sphere (CS) by 6 iron atoms. And in the second coordination sphere by 6 scandium atoms. This 12 iron and scandium atoms form a 12-vertex coordination around the iron atom [7].

As can be seen from Fig. 1a, the NMR spectrum of 45Sc in the $Fe_2Sc$ alloy has a single peak at the frequency 104.1 MHz and a hyperfine field equal to 100,8 kOe. A scandium atom in the cubic $MgCu_2$ lattice has a single crystallographic state and it has in its first CS 12 iron atoms and in its second CS 4 scandium atoms.

This 16 iron and scandium atoms form a 16-vertex coordination around the scandium atom [7]. The scandium atom is probably a non-magnetic atom in the $Fe_2Sc$ lattice. In this case, the hyperfine field at this atoms core, is due to the polarization of the spin density of conduction electrons due to magnetic moments of the 12 atoms next to it. The hyperfine field at the nucleus of 45Ss in $Fe_2Sc$ can be written as $H_0 = C_{Sc} * \mu_{Fe} * N$, where $C_{Sc}$ is the coupling constant and N the number of iron atoms in the first CS of the scandium atom (N = 12 ). Since, for this compound,the magnetic moment is $\mu_{Fe}$=1.43 $\mu_B$,the constant is $C_{Sc}$ =-5.87kOe (atom Fe)^-1*( $\mu_B$)^-1.

The NMR spectrum of the 57Fe alloy $Fe_2Sc$, containing excess iron atoms and having an $MgNi_2$ type structure, is composed of three resolved peaks at frequencies 24.1 ; 26.0 and 27.1 MHz (see Fig. 2). The ratio of the areas of these peaks is 1 : 0.7 : 1. The lattice $MgNi_2$ has three crystallographic nonequivalent states of iron atoms, Fe1, Fe2, and Fe3. The unit cell contains 24 atoms (16Fe and 8 Sc). The number N of iron atoms in each state in the unit cell is 6+6+4, and the number of scandium atoms is 4+4. Thus the resonance lines in the 57Fe spectrum of the $Fe_2Sc$ ($MgNi_2$) alloy are caused by the crystallographically different iron atoms. the ratio of the intensities of the NMR peak shows that the iron atoms, from which the nuclei resonate at 24.1 and 27.1 MHz, occupy the position in the cell with 6 iron atoms ( 6Fe1 and 6Fe2 ) and iron atoms, with core resonances at 26.0 MHz, occupy the state of the cell with the number n = 4 ( 4Fe2 ).
These three states of iron correspond to three hyperfine fields $H_1$= - 176.9 kOe ; $H_2$= -190.7 kOe and $H_3$= -198.7 kOe. Assuming that the coupling constant $A_{Fe}$ = -140 kOe / μv , we find that the local magnetic moments of the iron atoms in the crystallographically different states are μ1 = 1,26μB ; μ2 = 1,36μB and μ3 = = 1,42μB. The average magnetic moment of the iron in the $Fe_2Sc$ alloy with the $MgNi_2$ structure is 1,35μB. The NMR spectrum of 45Sc in the $Fe_{2.01}ScSs_{0.99}$ and the $Fe_{2.05}Sc_{0.95}$ alloy consisted of two allowed lines at 101.4 and 98.2 MHz, resulting in two crystallographically nonequivalent states of the scandium atoms in the $MgNi_2$ lattice, whereas the unit cell contains eight scandium atoms with a number N of atoms in each state( 4Sc1 + 4Sc2 ). A scandium atom is surrounded in its first CS by 12 iron atom and in in its second CS by 4 scandium atoms. This 16 Fe and Sc atoms form a 16-vertex around the scandium atom, this goes up for scandium atoms in a $MgCu_2$ lattice. Both different states of scandium have the same 12 Fe atoms in their first CS, but the hyperfine field of the 45Sc nuclei is not the same. This may be due to the fact that the 12 iron atoms surrounding scandium atoms have different magnetic moments. Indeed the state Sc1 contains in its first CS 6Fe1+3Fe2+3Fe3, whereas state Sc2 has 6Fe2+3Fe1+3Fe3. Assuming that for both states, the average hyperfine field is proportional to the average magnetic moment of the iron atoms, we evaluated the coupling constant $C_{Sc}$ for the $MgNi_2$ lattice. Since Ho = -96.6 kOe , and μFe = 1,35μB , the coupling constant is $C_{Sc}$ = -5.96 kOe • μB^-1• (atom Fe)^-1. Comparing these constants for the lattices $MgCu_2$ and $MgNi_2$, we see that they differ little from each other.

As noted above, the magnetization $\sigma$(T ) of the $Fe_2Sc$ alloy with structure MgNi2 and excess iron atoms has hysteresis in the temperature range 160-380 ° C, during heating and cooling. In this temperature range is also a deviation from linear growth of the lattice parameter with increasing temperature observed. The anomalous behavior of $\sigma$(T) and c(T) in this temperature range shows that there is a phase transition in the specified temperature range. A similar behavior of $\sigma$(T) and the lattice parameters is also found in Laves phase alloys of $Fe_2Hf_xTa_{1-x}$ for $(0.1 \leq x \leq 0.3)$, which also have a hexagonal structure [11]. In [11] it is shown that the observed features of the temperature dependences $\sigma$(T ) and the lattice parameter are due to the ferro – antiferromagnetic transitions, in accordance with the theory of magnetic phase transitions in the system of itinerant electrons, developed in [ 12 ]. We also observed similar hysteresis curves for the Fe – Sc alloys that differ from the stoichiometric $Fe_2Sc$ compound. In the alloys $Fe_2Hf_xTa_{1-x}$ $(0.1 \leq x \leq 0.3)$ occurs a transition from the ferromagnetic state of $Fe_2Hf$ to the antiferromagnetic state of $Fe_2Ta$, the exchange of hafnium atoms for the Ta atoms in this type of crystal induces the effect that some iron atoms become antiferromagnetic.

In the alloy $Fe_2Sc$ with a $MgNi_2$ type structure, an iron atom is surrounded in the first coordination sphere by 6 Fe atoms, and in the second CS by 6 Sc atoms. This 12 atoms for a 12-vertex around the iron atom. Around a scandium atom a 16-vertex is formed of 12 iron atoms (in the first CS) and 4 scandium atoms (in the second CS). In the alloys $Fe_{2.01}Sc_{0.99}$, $Fe_{2.05}Sc_{0.95}$ and others with a high content of additional iron atoms, the iron atoms occupy ‘wrong’ places, the places of the scandium atoms, forming, probably, antiferromagnetic Fe-Fe interactions. The most striking example of the weakening of ferromagnetic interaction and a strengthening of the antiferromagnetic interaction in Laves alloys is the quickly quenched (amorphous) $Fe_2Y$ alloy, because in this alloy competition between ferro- and antiferromagnetic interaction leads to the state of the “spin-glass” found in [13]. We believe that the appearance of antiferromagnetic interaction between Fe-Fe atoms in these alloys causes the hysteresis in $\sigma$(T) and the anomalous behavior of the lattice parameter c(T), in the temperature range 160-380 °C. The ferro- antiferromagnetic phase transition of the alloy $Fe_2Sc$ with $MgNi_2$ structure, and with an excess of iron atoms, can be qualitatively explained by the model of phase transitions described in [12]. Another qualitative explanation of the observed effects in the studied alloys may be the mechanism of magnetic transitions ,described in [14], where it is shown that a change of the type of (nearest) neighbor order, as in "order - order " or "order - a strange disorder", can also lead to a ferro - antiferromagnetic transition due to the difference in temperature dependence between Heisenberg and non-Heisenberg exchange interactions.

Institute of precision alloys
ЦНИИЧМ имени И. П. Бардив
received: 8-8-1985

## ЛИТЕРАТУРА


1. Наумкин О. П., Терехова В. Ф., Савицкий Е. М. Диаграмма состояния сплавов Fe—Sc. — Изв. АН СССР, Металлы, 1969, 3, с. 161—165.

2. Dwight A. E. Factors controlling the occurrence of Laves phases and $AB_5$ compounds among transition elements. — Trans. Amer. Soc. Metals, 1961, 53, p. 479—482.

3. Гладышевский Е. И., Крипякевич П. М., Протасов В. С. Вопросы теории и применения редкоземельных металлов. М.: Наука, 1964, с. 153.

4. Jkeda K., Nakamichi T., Yamada T., Yamomoto M. Ferromagnetism in $Fe_2Sc$ with hexagonal $MgZn_2$-type structure. — J. Phys. Soc. Japan, 1974, 36, p. 611.

5. Покатилов В. С., Садчиков В. В., Утенкова О. В. ЯМР исследование интерметаллического соединения $Fe_2S$. — ДАН СССР, 1985, 281, № 3, с. 574—577.

6. Stearns M. B. Spin echo and free induction decay measurements in pure Fe and Fe-rich ferromagnetic alloys. — Phys. Rev., 1967, 10, p. 496—509.

7. Теслюк М. Ю. Металлические соединения со структурами фаз Лавеса. М.: Наука, 1969, с. 10—17.

8. Oppelt A., Buschow K. N. J. NMR investigation of the hyperfine interaction in $Y(Fe_{1-x}A_x)_2$ ($A$=Al, Co, Pt). — Phys. Rev., 1976, 13, p. 4698—4704.

9. Weisinger G., Oppelt A., Buschow K. H. J. Hyperfine interactions and local magnetic ordering in $Zr(Fe_{1-x}Co_x)_2$ ($0 \leqslant x \leqslant 0{,}2$). — J. Magn. Mag. Mater., 1981, 22, p. 227—238.

10. Wallace W. Mossbauer effect measurements of hyperfine interactions in Laves phase containing Fe combined with Ti, Zr, Y and others. — J. Chem. Phys., 1964, 41, p. 3857—3863.

11. Nishihara Y., Yamaguchi Y. Magnetic phase transitions in itinerant electron magnets $Hf_{1-x}Ta_xFe$. — J. Phys. Soc. Japan, 1983, 52, p. 3630—3636.

12. Moriya T., Usami K. Coexistence of ferro-antiferromagnetism and phase transitions in itinerant electron systems. — Solid. State Comm., 1970, 23, p. 935—938.

13. Forester D. W. Localized moment and spin-glass-like behaivior in amorphous $YFe_2$. — Amorph. Magn., 1977, 2, p. 135—143.

14. Нагаев Э. Л., Коваленко А. А. Магнитные фазовые переходы «порядок — порядок» и «порядок — чужой беспорядок». — ЖЭТФ, 1980, 79, вып. 3(9), с. 907—921.

# Appendix B

*Tabel of compounds with the $MgNi_2$ crystal stucture, containing a magnetic transition metal*

Pearson database search criteria:

Phase prototype: MgNi2,hP24,194

Compound class: intermetallic

Structure class: Friauf-Laves phase

Containing magnetic elements

| **Chemical system Phase formula** | **Production method** | **Magnetic properties** | |
|---|---|---|---|
| Al-Co-Nb $Nb_{0.8}Co_2Al_{0.2}$ | *crucible-free levitation melting in an argon and drop-casting into cold copper molds.<br>*or arc-melting under argon<br>*different heat-treatments in the range 800-1150 | Not in article | http://www.sciencedirect.com/science/article/pii/S0966979510002955 |
| Al-Co-Ta $Ta_{0.6}Co_2Al_{0.4}$ | *mixed powders were arc-melted, several times re-melted, under argon<br>*annealed at 1173-1473 K for 170 h under vacuum | Not in article | http://www.sciencedirect.com/science/article/pii/0022508889902348 |
| Al-Mg-Ni $Mg_{0.95}Ni_{1.79}Al_{0.26}$ | *Powders were mixed at 150 rpm for 1 hour. Pressed into 10mm pellets at 300MPa, which were sealed in iron tubes under argon.<br>*Annealed at 700 ºC for 20 days.<br>*Alloys with a high amount of Ni were first sintered at 0.7-0.85 melting temperature and annealed for 25 days at 427ºC. | Not in article | http://www.hanser-elibrary.com/doi/pdf/10.3139/146.101719 |
| Co-Nb $Nb_{1.25}Co_{1.75}$ht | *Arc-melted under argon<br>*Annealed at 1573 ºC | Not in article | Metastable phases in the cobalt-niobium system |
| Co-Ni-Ti $Ti_{0.92}Co_2Ni_{0.08}$ | *Arc-melted under argon<br>*Annealed at 900 ºC for a week in evacuated silica tubes | Not in article | http://www.sciencedirect.com/science/article/pii/0022508881902691 |
| Co-Ta $Ta_{0.8}Co_{2.2}$ rt | powder metallurgical technique | Not in article | The phase diagram of the Co-Mo-Ta system at 1000 °C |

| | | | |
|---|---|---|---|
| Co-Ti<br>$Ti_{0.9}Co_{2.1}$ | *Arc-melted under argon<br>* Annealed at 1173 ºC for a week in evacuated silica tubes | Not in article | http://www.sciencedirect.com/science/article/pii/0022508881902691 |
| Co-Y-Zr<br>$Y_{0.14}Zr_{0.55}Co_2$ | *Arc-melted, several times re-melted.<br>*Annealed at 1073 K for 2 w in evacuated silica tube (sample wrapped in tantalum foil) | Ferromagnetic. Magnetization and Tc increase temperature with increasing Y content, until a max of 300 K<br>argon<br>annealed at 1073 K for 2 w in evacuated silica tub<br>wrapped in tantalum foil) | http://journals.jps.jp/doi/pdf/10.1143/JPSJ.55.4435 |
| Cr-Fe-Zr<br>$ZrCr_{1.949}Fe_{0.051}$ | *arc-melted under argon<br>* annealed at 1773 K for 1 h, quenched into liquid gallium | Russian, not available | Interaction of the metallic compound $ZrCr_2$ with some compounds of zirconium with iron, cobalt and nickel |
| Cr-Hf<br>$HfCr_2$ | *arc-melted under argon<br>* annealed at 1773 K for 1 h, quenched into liquid gallium | Article not available | The Laves phases in hafnium alloyed with group IV transition metals |
| Cr-Mn-Zr<br>$ZrCr_{1.949}Fe_{0.051}$ | *arc-melted under argon<br>* annealed at 1673 K for 25 h under argon | Russian, not available | Interaction of the Laves phases in the systems $ZrMn_2$-$ZrCu_2$ and $ZrMn_2$-$ZrV_2$ |
| Cr-Ta<br>$Ta_{1.2}Cr_{1.8}$ rt | | Russian, not available | Phase equilibria<br>and crystal<br>structures of the<br>intermediate phases in the system Ta-Cr |
| Cr-Ti<br>$Cr_2Ti$ ht2 | Melted several times with induction melting under argon | Not in article | http://www.sciencedirect.com/science/article/pii/S0925838802000130?np=y |

| | | | |
|---|---|---|---|
| Cr-Zr<br>$Cr_2$ ht1 | Arc-melted 6 times, under argon | Not in article | http://www.sciencedirect.com/science/article/pii/S002236971100240X |
| Cu-Mg-Ni<br>$Cu_{0.14}Zr_{0.55}Co_2$ | *Melting the powders in an argon-filled induction furnace<br>*Annealed for 5 d at 400 ºC in argon-filled silica tubes | Not in article | http://journals.iucr.org/b/issues/1972/03/00/a08954/a08954.pdf |
| Fe-Hf<br>$Fe_2Hf$ ht2 | *Arc-melted under argon<br>*annealed at 1173 K for 200 h in sealed evacuated quartz tube, quenched | Russian, not available | Interaction of Laves Phases in the Systems $Zr(Fe,Co,Ni)_2$-$Hf(Fe,Co,Ni)_2$ |
| Fe-Ni-Y<br>$FeNiY$ ht | *Arc-melted several times<br>*Annealed for several days. | Itinerant electromagnetism in cubic C15 phases | http://www.sciencedirect.com/science/article/pii/0022508869900368 |
| Fe-Ru-Sc<br>$ScFe_{1.5}Ru_{0.5}$ | *Melted<br>*Annealed at 873 K for 400 h, quenched to 273 K | Article not available | Reactions of $ScFe_2$ doped with yttrium, ruthenium, and gallium with nitrogen in the presence of hydrogen |
| Fe-Sb-Zr<br>$ZrFe_{1.7}Sb_{0.3}$ Fe+ | *Arc-melted<br>*Annealed at 1173 K for 14 d | Not in article | http://www.sciencedirect.com/science/article/pii/S0966979510002992 |
| Fe-Sc<br>$Fe_{2.05}Sc_{0.95}$ ht1 | *Arc-melted<br>*Annealed at 950 ºC for 30 h, furnace-cooled | *Itinerant ferromagnetic<br>*For the non-stoichiometric compounds a first-order phase transition is observed from the ferro- to the antiferromagnetic phase, around 380 ºC. | Structure and magnetic properties of Fe-Sc alloys<br>Phys. Met. Metallogr. (1986) 62, 1, 59-65<br>Fiz. Met. Metalloved. (1986) 62, 69-75 |
| Fe-Zn-Zr<br>$Zr_{0.66}Fe_{2.05}Sn_{0.3}$ | *Arc-melted<br>*Annealed at 1173 K for 14 d in evacuated silica tube. | Not in article | http://www.sciencedirect.com/science/article/pii/S0966979510002992 |
| Fe-Zr<br>$Fe_2Zr$ Fe+ | *Arc-melted<br>*Annealed at 1373 K for 72 h under vacuum, furnace-cooled | For the MgNi2 variant with excess iron, Tc is at 700 ºC, and the saturation magnetisation 120 emu/gr | http://journals.jps.jp/doi/pdf/10.1143/JPSJ.25.1192 |

| | | | |
|---|---|---|---|
| Hf-Mn<br>$Mn_2Hf$ hex2 | *Arc-melted<br>*Inert atmosphere | Article not available | The occurrence of Laves-type phases among transition elements |
| La-Mg-Ni<br>$Mg_{0.98}La_{0.02}Ni_2$ | *Melted in induction furnace, for 3 times, while shaking the crucibles repeatedly<br>*Annealed at 773 K for 21 d in alumina crucible inside tantalum tube in sealed evacuated quartz tube, quenched | Not in article | http://www.sciencedirect.com/science/article/pii/S092583880601334X |
| Mg-Ni<br>$Ni_2Mg$ | *Melted in argon filled induction furnace<br>*Annealed at 673 K for 5 d | Not in article | http://journals.iucr.org/b/issues/1972/03/00/a08954/a08954.pdf |
| Mg-Ni-Zn<br>$MgZn_{0.42}Ni_{1.58}$ | *Melted in argon filled induction furnace<br>*Annealed at 673 K for 5 d | Not in article | http://journals.iucr.org/b/issues/1972/03/00/a08954/a08954.pdf |
| Mn-V-Zr<br>$ZrV_{0.9}Mn_{1.1}$ | *Arc-melted<br>*Annealed at 1423 K for 200 h under argon | Russian, not available | Interaction of the Laves phases in the systems $ZrMn_2$-$ZrCu_2$ and $ZrMn_2$-$ZrV_2$ |